AFRL-SR-AR-TR-05-

REPORT DOCUMENTATION PAGE

0106

1. AGENCY USE ONLY (Leave blank)	2. REPORT DATE	3. REPORT TYPE AND DATES COVERED
	March 3, 2005	Final Report 30Sep2003 – 29Sep2004

4. TITLE AND SUBTITLE
General Electric Research Team Mathematics Project

5. FUNDING NUMBERS
F49620-03-1-0439

6. AUTHOR(S)
Anthony T. Patera

7. PERFORMING ORGANIZATION NAME(S) AND ADDRESS(ES)
Massachusetts Institute of Technology
Dept. of Mechanical Engineering
Room 3-266
77 Massachusetts Avenue
Cambridge, MA 02139

8. PERFORMING ORGANIZATION REPORT NUMBER

9. SPONSORING / MONITORING AGENCY NAME(S) AND ADDRESS(ES)
Air Force Office of Scientific Research
AFOSR/NM
4015 Wilson Blvd., Room 713
Arlington, VA 22203-1954

10. SPONSORING / MONITORING AGENCY REPORT NUMBER
N/A

11. SUPPLEMENTARY NOTES

12a. DISTRIBUTION / AVAILABILITY STATEMENT
Approved for public release;
Distribution unlimited.

12b. DISTRIBUTION CODE

13. ABSTRACT *(Maximum 200 Words)*

This research was directed at strengthening DARPA's Prognosis initiative by including new mathematical methods for managing uncertainty during the design, application, and prediction of the behavior of structural materials. The research program consisted of three projects carried out by Yale University, Massachusetts Institute of Technology, and the [illegible]. The projects were: (1) Yale — Multiscale geometric analysis in high-dimensional spaces; (2) MIT — Reliable fast parameter estimation and (e.g., process or mission) optimization in the presence of uncertainty; and (3) MIT/Caltech — Exact bounds and certificates for functional outputs of solutions of the partial differential equations of continuum mechanics.

14. SUBJECT TERMS
Structural materials, design of materials; optimization; parameter estimation; uncertainty quantification; continuum mechanics; partial differential equations; output bounds

15. NUMBER OF PAGES
28

16. PRICE CODE

17. SECURITY CLASSIFICATION OF REPORT	18. SECURITY CLASSIFICATION OF THIS PAGE	19. SECURITY CLASSIFICATION OF ABSTRACT	20. LIMITATION OF ABSTRACT
Unclassified	Unclassified	Unclassified	SAR

NSN 7540-01-280-5500

Standard Form 298 (Rev. 2-89)
Prescribed by ANSI Std. Z39-18
298-102

General Electric Research Team Mathematics Project

Grant Number F49620-03-1-0439

Anthony T. Patera
Department of Mechanical Engineering
Massachusetts Institute of Technology

Background

This research was directed at strengthening DARPA's Prognosis initiative by including new mathematical methods for managing uncertainty during the design, application, and prediction of the behavior of structural materials. The research program consisted of three projects carried out by Yale University, Massachusetts Institute of Technology, and the California Institute of Technology. These projects were: (1) Yale — Multiscale geometric analysis in high-dimensional spaces; (2) MIT — Reliable fast parameter estimation and (e.g., process or mission) optimization in the presence of uncertainty; and (3) MIT/Caltech — Exact bounds and certificates for functional outputs of solutions of the partial differential equations of continuum mechanics.

Project 1 — Applying Multiscale Geometric Analysis in High-Dimentional Space

Investigator: Peter W. Jones
Department of Mathematics
11 Hillhouse Avenue
PO Box 208283
Yale University
New Haven, CT 06520-8283

Final report not provided.

Project 2 — Reliable Fast Optimization in the Presence of Uncertainty

Project 2(a):

Investigator: Dimitris Bertsimas
Operations Research Center
Sloan School of Management
Room E53-363
Massachusetts Institute of Technology
Cambridge, MA 02139

Final report not provided.

Project 2(b):

Certified Rapid Solution of Parametrized Partial Differential Equations for Real-Time Applications[1]

Investigator: Anthony T. Patera
Department of Mechanical Engineering
77 Mass. Ave., Room 3-266
Massachusetts Institute of Technology
Cambridge, MA 02139

1 Introduction

Engineering analysis requires the prediction of selected "outputs" s relevant to ultimate component and system performance; typical outputs include critical stresses or strains, flowrates or pressure drops, and various measures of temperature and heat flux. These outputs are functions of "inputs" μ that serve to identify a particular configuration of the component or system; typical inputs reflect geometry, properties, and boundary conditions and loads.

In many cases, the input-output function is best articulated as a (say) linear functional ℓ of a field variable $u(\mu)$ that is the solution to an input-parametrized partial differential equation (PDE); typical field variables and associated PDEs include temperature and steady/unsteady conduction, displacement and equilibrium elasticity/Helmholtz, and velocity and steady incompressible Navier-Stokes. System behavior is thus described by an input-output relation $s(\mu) = \ell(u(\mu))$ the evaluation of which requires solution of the underlying PDE.

Our focus is on "deployed" systems — components or processes *in operation* in the field — and associated "Assess-Act" scenarios. In the Assess stage we pursue robust parameter estimation (inverse) procedures that map measured-observable outputs to (all) possible system-characteristic and environment-state inputs. In the subsequent Act stage we then pursue adaptive design (optimization) procedures that map mission-objective outputs to best control-variable inputs. The computational requirements on the PDE-induced evaluation $\mu \rightarrow s$ are formidable: the response must be *real-time* — we must "Assess-Act" *immediately*; and the outputs must be rigorously *certified* — we must "Assess-Act" *safely* and *feasibly* [23].

In this project, we develop a method for real-time certified evaluation of PDE input-output relations; the two ingredients are reduced-basis (RB) approximation [2, 8, 9, 12, 18, 22, 24, 25] and *a posteriori* error estimation [18, 21, 27, 34, 35, 36]. We also consider the incorporation of these methods in the Assess-Act paradigm with particular application to problem areas of interest to DARPA and GE: in particular, "prognostics" and "accelerated insertion of materials." In Sections 2–4 we describe the basic methodology for a relatively simple class of problems — linear elliptic equations; and in Section 5 we apply this technology to a non-destructive-testing example — on-line crack detection — relevant to ultimate prognostics systems. In Section 6 and Section 7 we extend the methodology to two classes of problems relevant to accelerated insertion of materials (and materials processing): in Section 6 we consider the equations of fluid flow; and in Section 7 the equations of time-dependent heat transfer (e.g., relevant to turbine disk quenching). We note that, due to the short duration of this project, we have not yet applied the full Assess-Act paradigm to the models of Sections 6 and 7; however, this will be pursued in future work.

[1] Based on invited paper submitted to Volume on 2nd Sandia Workshop on PDE-Constrained Optimization: Toward Real-Time and Online PDE-Constrained Optimization.

2 Abstract Statement: Elliptic Linear Equations

We first consider the "exact" (superscript e) problem: given $\mu \in \mathcal{D} \subset \mathbb{R}^P$, we evaluate $s^e(\mu) = \ell(u^e(\mu))$, where $u^e(\mu)$ satisfies the weak form of our μ-parametrized PDE, $a(u^e(\mu), v; \mu) = f(v)$, $\forall\, v \in X^e$. Here μ and $\mathcal{D}$ are the input and (closed) input domain, respectively; $u^e(\mu)$ is our field variable; X^e is a Hilbert space with inner product (w, v) and associated norm $\|w\| = \sqrt{(w, w)}$; and $a(\cdot, \cdot; \mu)$ and $f(\cdot)$, $\ell(\cdot)$ are X^e-continuous bilinear and linear functionals, respectively.

Our interest here is in second-order PDEs, and thus $(H_0^1(\Omega))^\nu \subset X^e \subset (H^1(\Omega))^\nu$; here $\Omega \subset \mathbb{R}^d$ is our spatial domain, $\nu = 1$ for a scalar field variable and $\nu = d$ for a vector field variable; and $H^1(\Omega)$ (respectively, $H_0^1(\Omega)$) is the usual Hilbert space of derivative square-integrable functions (respectively, derivative square-integrable functions that vanish on the domain boundary, $\partial\Omega$) [28]. The associated inner product $(\cdot, \cdot)$ is a μ-independent continuous coercive symmetric bilinear form over X^e that perforce induces an $(H^1(\Omega))^\nu$-equivalent norm $\|\cdot\|$.

We next introduce X (typically, $X \subset X^e$), a reference finite element approximation space of finite dimension $\mathcal{N}$. Our reference (or "truth") finite element approximation $u(\mu) \in X$ is then defined by $a(u(\mu), v; \mu) = f(v)$, $\forall\, v \in X$: $u(\mu) \in X$ is a calculable surrogate for $u^e(\mu)$ upon which we will build our RB approximation and with respect to which we will evaluate the RB error; $u(\mu)$ also serves as the "classical alternative" relative to which we will assess the efficiency of our approach. We assume that $\|u^e(\mu) - u(\mu)\|$ is suitably small and hence that $\mathcal{N}$ is typically very large: our formulation must be both *stable* and *efficient* as $\mathcal{N} \to \infty$.

We shall make two crucial hypotheses. The first hypothesis is related to well-posedness, and is often verified only *a posteriori*. We assume that the inf-sup parameter, $\beta(\mu) \equiv \inf_{w \in X} \sup_{w \in X} [a(w, v; \mu)/(\|w\|\|v\|)]$, is strictly positive: $\beta(\mu) \geq \beta_0 > 0$, $\forall\, \mu \in \mathcal{D}$. The second hypothesis is related primarily to numerical efficiency, and is typically verified *a priori*. We assume that a is *affine* in the parameter μ: $a(w, v; \mu) = \sum_{q=1}^{Q} \Theta^q(\mu) a^q(w, v)$, for $q = 1, \ldots, Q$ parameter-*dependent* functions $\Theta^q(\mu) : \mathcal{D} \to \mathbb{R}$ and parameter-*independent* continuous bilinear forms $a^q(w, v)$. The affine assumption may in fact be relaxed [5].

3 Reduced-Basis Approximation

The reduced-basis (RB) approximation was first introduced in the late 1970s in the context of nonlinear structural analysis [2, 22] and subsequently abstracted and analyzed [8, 25] and extended [9, 12, 24] to a much larger class of parametrized partial differential equations. We first introduce nested samples $S_N = \{\mu_1 \in \mathcal{D}, \ldots, \mu_N \in \mathcal{D}\}$, $1 \leq N \leq N_{\max}$, and associated nested "Lagrangian" RB spaces $W_N \equiv \text{span}\,\{\zeta_n(\mu_n) \equiv u(\mu_n),\ 1 \leq n \leq N\}$, $1 \leq N \leq N_{\max}$. Our RB approximation is then: given $\mu \in \mathcal{D}$, evaluate $s_N(\mu) = \ell(u_N(\mu))$, where $u_N(\mu)$ satisfies $a(u_N(\mu), v; \mu) = f(v)$, $\forall\, v \in W_N$. We consider here only Galerkin projection.

In essence, W_N comprises "snapshots" on the parametrically induced manifold $\mathcal{M} \equiv \{u(\mu) \,|\, \mu \in \mathcal{D}\} \subset X$. It is clear that $\mathcal{M}$ is very *low-dimensional*; furthermore, it can be shown under our hypotheses — we consider the equations for the sensitivity derivatives and invoke stability and continuity — that $\mathcal{M}$ is very *smooth*. We thus anticipate that $u_N(\mu) \to u(\mu)$ very rapidly, and hence that — at least for modest P — we may choose $N \ll \mathcal{N}$. Many numerical examples justify this expectation (see Sections 5, 6, and 7); and, in certain simple cases, exponential convergence can be proven [19]. We emphasize that the deployed context requires global reduced-basis approximations that are *uniformly* (rapidly) convergent over the entire parameter domain $\mathcal{D}$; proper choice of the parameter samples S_N is thus crucial (see Section 4).

We now represent $u_N(\mu)$ as $u_N(\mu) = \sum_{j \in \mathbb{N}} u_{Nj}(\mu) \zeta_j$, where $\mathbb{N} \equiv \{1, \ldots, N\}$, and $\mathbb{N}_{\max} \equiv \{1, \ldots, N_{\max}\}$. Our RB output may then be expressed as $s_N(\mu) = \sum_{j \in \mathbb{N}} u_{Nj}(\mu) \ell(\zeta_j)$, where — we now invoke our affine assumption — the $u_{Nj}(\mu)$, $1 \leq j \leq N$, satisfy the $N \times N$ linear algebraic

system

$$\sum_{j\in\mathbb{N}} \Big\{ \sum_{q\in\mathbb{Q}} \Theta^q(\mu) a^q(\zeta_j,\zeta_i) \Big\} u_{N\,j}(\mu) = f(\zeta_i), \quad \forall\, i \in \mathbb{N}\,, \tag{1}$$

where $\mathbb{Q} \equiv \{1,\ldots,Q\}$. (In practice we replace the ζ_j, $1 \le j \le N$, with a $(\cdot,\cdot)$-orthonormalized system; the algebraic stiffness matrix is then well-conditioned.) It is clear from (1) that we may pursue an offline-online computational strategy [3, 12, 18, 27] ideally suited to the deployed real-time context.

In the *offline* stage — performed *once* — we first solve for the ζ_i, $\forall\, i \in \mathbb{N}_{\max}$; we then form *and store* $\ell(\zeta_i)$, $\forall\, i \in \mathbb{N}_{\max}$, and $a^q(\zeta_j,\zeta_i)$, $\forall\, (i,j) \in \mathbb{N}^2_{\max}$, $\forall\, q \in \mathbb{Q}$. In the online stage — performed many times, for each new μ "in the field" — we first assemble and subsequently invert the (full) $N \times N$ "stiffness" matrix $\sum_{q\in\mathbb{Q}} \Theta^q(\mu) a^q(\zeta_j,\zeta_i)$ to obtain the $u_{N\,j}(\mu)$, $1 \le j \le N$ — at cost $O(QN^2) + O(N^3)$; we then evaluate the sum $\sum_{j\in\mathbb{N}} u_{N\,j}(\mu)\ell(\zeta_j)$ to obtain $s_N(\mu)$ — at cost $O(N)$. The online complexity is *independent* of $\mathcal{N}$, and hence — given that $N \ll \mathcal{N}$ — we shall realize extremely rapid "deployed" response.

4 A Posteriori Error Estimation

We first "presume" $\tilde{\beta}(\mu)$, a (to-be-constructed) positive lower bound for the inf-sup parameter, $\beta(\mu)$: $\beta(\mu) \ge \tilde{\beta}(\mu) \ge \tilde{\beta}_0 > 0$, $\forall\, \mu \in \mathcal{D}$. We next introduce the dual norm of the residual: $\varepsilon_N(\mu) \equiv \sup_{v\in X} [R(v;\mu)/\|v\|]$, where $R(v;\mu) \equiv f(v) - a(u_N(\mu),v;\mu)$, $\forall\, v \in X$.

We may now define our error estimator, $\Delta_N(\mu) \equiv \varepsilon_N(\mu)/\tilde{\beta}(\mu)$, and associated effectivity, $\eta_N(\mu) \equiv [\Delta_N(\mu)/\|u(\mu) - u_N(\mu)\|]$. We can then readily demonstrate [27, 36] that

$$1 \le \eta_N(\mu) \le \gamma(\mu)/\tilde{\beta}(\mu), \quad \forall\, \mu \in \mathcal{D},\ \forall\, N \in \mathbb{N}_{\max}, \tag{2}$$

where $\gamma(\mu) \equiv \sup_{w\in X} \sup_{v\in X} [a(w,v;\mu)/(\|w\|\|v\|)]$ is our continuity "constant." The left inequality states that $\Delta_N(\mu)$ is a *rigorous* upper bound for $\|u(\mu) - u_N(\mu)\|$; the right inequality states that $\Delta_N(\mu)$ is a (reasonably) *sharp* upper bound.

We may also develop bounds for the error in the output; we consider here the special "compliance" case in which $\ell = f$ and a is symmetric — more general functionals ℓ and nonsymmetric a require adjoint techniques [27]. We first define our output error estimator, $\Delta^s_N(\mu) \equiv \varepsilon^2_N(\mu)/\tilde{\beta}(\mu)$, which scales as the *square* of the dual norm of the residual, $\varepsilon_N(\mu)$. We can then demonstrate [21, 27, 36] that $1 \le \Delta^s_N(\mu)/|s(\mu) - s_N(\mu)|$, $\forall\, \mu \in \mathcal{D}$, $\forall\, N \in \mathbb{N}_{\max}$ — $\Delta^s_N(\mu)$ is a rigorous upper bound for $|s(\mu) - s_N(\mu)|$; we may further prove [27] in the coercive case that $\Delta^s_N(\mu)/|s(\mu) - s_N(\mu)| \le \gamma(\mu)/\tilde{\beta}(\mu)$ — $\Delta^s_N(\mu)$ is a (reasonably) sharp upper bound.

It remains to develop appropriate constructions and associated offline-online computational procedures for the efficient calculation of $\varepsilon_N(\mu)$ and $\tilde{\beta}(\mu)$. To begin, we consider the former [18, 21, 27]: we invoke duality, our reduced-basis expansion, the affine parametric dependence of a, and linear superposition to express

$$\varepsilon^2_N(\mu) = (\mathcal{C},\mathcal{C}) + \sum_{q\in\mathbb{Q}} \sum_{n\in\mathbb{N}} \Theta^q(\mu) u_{N\,n}(\mu) \{2(\mathcal{C},\mathcal{L}^q_n) + \sum_{q'\in\mathbb{Q}} \sum_{n'\in\mathbb{N}} \Theta^{q'}(\mu) u_{N\,n'}(\mu) (\mathcal{L}^q_n, \mathcal{L}^{q'}_{n'})\},$$

where $\mathcal{C} \in X$ and $\mathcal{L}^q_n \in X$, $\forall\, n \in \mathbb{N}$, $\forall\, q \in \mathbb{Q}$ satisfy the *parameter-independent* Poisson(-like) problems $(\mathcal{C},v) = f(v)$, $\forall\, v \in X$ and $(\mathcal{L}^q_n, v) = -a^q(\zeta_n, v)$, $\forall\, v \in X$.

An efficient offline-online decomposition may now be identified. In the offline stage — performed only once — we first solve for $\mathcal{C}$ and $\mathcal{L}^q_n$, $\forall n \in \mathbb{N}_{\max}$, $\forall q \in \mathbb{Q}$; we then form *and store* the associated parameter-independent inner products $(\mathcal{C},\mathcal{C})$, $(\mathcal{C},\mathcal{L}^q_n)$, $(\mathcal{L}^q_n,\mathcal{L}^{q'}_{n'})$, $\forall\, (n,n') \in \mathbb{N}^2_{\max}$, $\forall\, (q,q') \in \mathbb{Q}^2$. In the online stage — performed many times, for each new value of μ "in the field" — we simply

evaluate the $\varepsilon_N^2(\mu)$ sum in terms of $\Theta^q(\mu)$, $u_{Nn}(\mu)$, and the precomputed inner products — at cost $O(Q^2N^2)$. The online cost is *independent* of $\mathcal{N}$ and — for Q not too large — commensurate with the online cost to evaluate $s_N(\mu)$.

Finally, we turn to the development of our lower bound $\tilde{\beta}(\mu)$ for the inf-sup "constant" $\beta(\mu)$. For simplicity, we consider here the particular case $P = 1$, $Q = 2$, $\Theta^1(\mu) = 1$, $\Theta^2(\mu) = \mu$: $a(w, v; \mu) = a^1(w, v) + \mu a^2(w, v)$; we further suppose that $\mathcal{D}$ is convex. The more difficult general case is considered in [21] and illustrated in subsequent sections. As our point of departure, we note that $\beta(\mu) \equiv \inf_{v \in X} \sqrt{b(v, v; \mu)/\|v\|^2}$, where $b(w, v; \mu) = (T^\mu w, T^\mu v)$, $\forall\, w, v \in X$, and $w \in X \rightarrow T^\mu w \in X$ is defined as $(T^\mu w, v) = a(w, v; \mu)$, $\forall\, v \in X$.

Next, given any $\overline{\mu} \in \mathcal{D}$ and constant $\bar{\epsilon} \in]0, 1[$, we introduce $t(w, v; \mu; \overline{\mu}) \equiv b(w, v; \overline{\mu}) + (\mu - \overline{\mu})[a^2(w, T^{\overline{\mu}} v) + a^2(v, T^{\overline{\mu}} w)]$ and $\mathcal{D}^{\overline{\mu}} \equiv \{\mu \in \mathcal{D} \,|\, t(v, v; \mu; \overline{\mu}) \geq 0\}$. We may then define $\tau(\mu; \overline{\mu}) \equiv \inf_{v \in X} \sqrt{t(v, v; \mu; \overline{\mu})/\|v\|^2}$, $\forall\, \mu \in \mathcal{D}^{\overline{\mu}}$. Our function $\tau(\mu; \overline{\mu})$ enjoys three properties: (i) $\beta(\mu) \geq \tau(\mu; \overline{\mu}) \geq 0$, $\forall\, \mu \in \mathcal{D}^{\overline{\mu}}$; (ii) $\tau(\mu; \overline{\mu})$ is concave in μ over the convex domain $\mathcal{D}^{\overline{\mu}}$; and (iii) $\tau(\mu; \overline{\mu})$ is "tangent" to $\beta(\mu)$ at $\mu = \overline{\mu}$. (To make property (iii) rigorous we must in general consider non-smooth analysis and also possibly a continuous spectrum as $\mathcal{N} \rightarrow \infty$.)

We can now develop our inf-sup lower bound $\tilde{\beta} : \mathcal{D} \rightarrow \mathbb{R}$. We first require a sample $E_J \equiv \{\overline{\mu}_1 \in \mathcal{D}, \ldots, \overline{\mu}_J \in \mathcal{D}\}$ and associated set of polytopes $C_J \equiv \{\mathcal{P}_1 \subset \mathcal{D}^{\overline{\mu}_1}, \ldots, \mathcal{P}_J \subset \mathcal{D}^{\overline{\mu}_J}\}$ that satisfy (a) a "Positivity Condition," $\tau(\mu; \overline{\mu}_j) \geq \bar{\epsilon}\, \beta(\overline{\mu}_j)$, $\forall\, \mu \in \mathcal{P}_j, 1 \leq j \leq J$, and (b) a "Coverage Condition," $\mathcal{D} \subset \cup_{j=1}^J \mathcal{P}_j$; we may then define

$$\tilde{\beta}(\mu) \equiv \max_{\{j \in \{1, \ldots, J\} \,|\, \mu \in \mathcal{P}_j\}} \bar{\epsilon}\, \beta(\overline{\mu}_j). \tag{3}$$

(We can also develop piecewise *linear* approximations, though — as discussed further in Section 5 — our inf-sup lower bound need not be highly accurate.) It is readily demonstrated that $\tilde{\beta}(\mu)$ has the requisite theoretical and computational attributes: $\beta(\mu) \geq \tilde{\beta}(\mu) \geq \bar{\epsilon}\, \beta_0 > 0$, $\forall\, \mu \in \mathcal{D}$; the online complexity $\mu \rightarrow \tilde{\beta}(\mu)$ depends only (and at most linearly) on J, which in turn depends only on P and Q and *not* on $\mathcal{N}$. Properties (i), (ii), and (iii) permit us to parlay relatively few expensive (offline) evaluations into a very inexpensive global (online) lower bound.

As an illustrative example we consider the Helmholtz-elasticity crack example of the next section for $\mu = (\omega^2 \in [2.5, 5.0], z = 1.0, L = 0.2)$ — the crack location, z, and crack length, L, are fixed, and only the frequency squared, ω^2, is permitted to vary — and material damping coefficient $d_m = 0.1$. We find that a sample $E_{J=3}$ suffices to satisfy our Positivity and Coverage Conditions for $\bar{\epsilon} = 0.4$. We present in Figure 1(a) $\beta(\mu)$; $\tau(\mu; \overline{\mu}_j)$ for $\mu \in \mathcal{D}^{\overline{\mu}_j}, 1 \leq j \leq J$; and our lower bound (3). We note that $\beta(\mu)$ is not concave (or convex) or even quasi-concave, and hence $\tau(\mu; \overline{\mu})$ is a necessary intermediary in the construction of our lower bound.

In conclusion, we can calculate a rigorous and sharp upper bound for $|s(\mu) - s_N(\mu)|$, $\Delta_N^s(\mu) \equiv \varepsilon_N^2(\mu)/\tilde{\beta}(\mu)$, with online complexity *independent* of $\mathcal{N}$. These inexpensive error bounds serve most crucially in the deployed stage — to choose optimal N, to confirm the desired accuracy, to establish strict feasibility, and to control sub-optimality. However, the bounds may also be gainfully enlisted in the pre-deployed stage — to construct optimal samples S_N [21, 36]: Given $S_1^{\text{opt}} = \mu_1^*$ [DO $N = 2, \ldots, N_{\max}$; $\mu_N^* = \arg\max_{\mu \in \Xi^F} \Delta_{N-1}^s(\mu)$; $S_N^{\text{opt}} = S_{N-1}^{\text{opt}} \cup \mu_N^*$; END]; our input sample Ξ^F can be large since the marginal cost to evaluate $\Delta_N^s(\mu)$ is small. (In contrast to POD economization procedures [31] *we never form the rejected snapshots*: our inexpensive bound $\Delta_N^s(\mu)$ serves as a (good) surrogate for the actual error.)

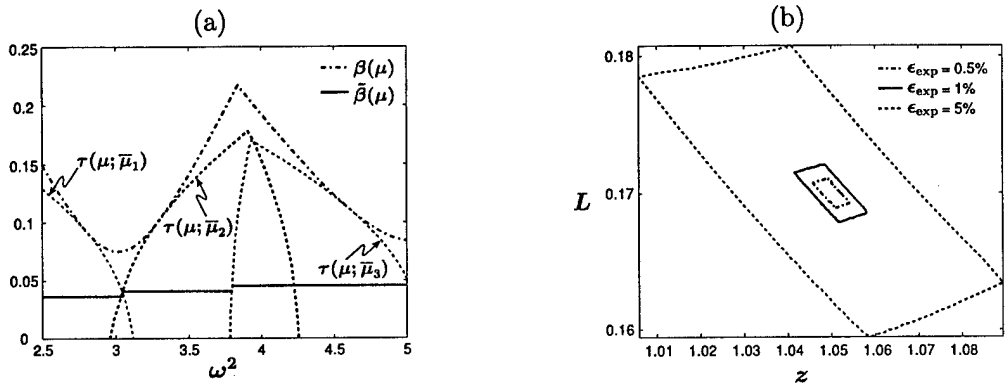

Figure 1: Helmholtz-elasticity example: (a) Plots of $\beta(\mu)$; $\tau(\mu;\overline{\mu}_j)$ for $\mu \in \mathcal{D}^{\overline{\mu}_j}, 1 \le j \le J$; and $\tilde{\beta}(\mu)$. (b) Crack parameter uncertainty region $\mathcal{R}$.

5 Assess-Act Example: Helmholtz-Elasticity

We apply the RB method here to a Helmholtz-elasticity equation often encountered in solid mechanics: inverse analyses based on the Helmholtz-elasticity PDE can gainfully serve in non-destructive evaluation (NDE) procedures for crack characterization [10, 15, 17] and damage assessment [13, 16]. The RB method significantly improves the efficiency of these inverse procedures — accelerating the *many* evaluations [14] of the PDE outputs.

We consider a two-dimensional thin plate with a horizontal crack at the (say) interface of two lamina: the (original) domain $\Omega^o(z, L) \subset \mathbb{R}^2$ is defined as $[0,2] \times [0,1] \setminus \Gamma^o_C$, where $\Gamma^o_C \equiv \{x_1 \in [z - L/2, z + L/2], x_2 = 1/2\}$ defines the idealized crack. The left surface of the plate is secured; the top and bottom boundaries are stress-free; and the right boundary is subject to a vertical oscillatory uniform force of frequency ω. We model the plate as plane-stress linear isotropic elastic with (scaled) density unity, Young's modulus unity, and Poisson ratio 0.25; the latter determine the (parameter-independent) constitutive tensor $E_{ijk\ell}$. Our input is $\mu \equiv (\mu_{(1)}, \mu_{(2)}, \mu_{(3)}) \equiv (\omega^2, z, L)$; our output is the (oscillatory) amplitude of the average vertical displacement on the right edge of the plate.

The governing equation for the displacement $w^o(x^o; \mu) \in X^o(\mu)$ is therefore $a^o(w^o(\mu), v; \mu) = f^o(v), \forall v \in X^o(\mu)$, where $X^o(\mu)$ is a quadratic finite element truth approximation subspace (of dimension $\mathcal{N} = 14{,}662$) of $X^e(\mu) = \{v \in (H^1(\Omega^o(z, L)))^2 \,|\, v|_{x^o_1=0} = 0\}$; $a^o(w, v; \mu) \equiv \int_{\Omega^o(z,L)} w_{i,j} E_{ijk\ell} v_{k,\ell} - \omega^2 w_i v_i$ ($v_{i,j}$ denotes $\partial v_i / \partial x_j$ and repeated physical indices imply summation); and $f^o(v) \equiv \int_{x^o_1=2} v_2$. The crack surface is hence modeled extremely simplistically — as a stress-free boundary. (No crack-tip element is needed as the output of interest is far from the crack.) The output $s^o(\mu)$ is given by $s^o(\mu) = \ell(u^o(\mu))$, where $\ell^o(v) = f^o(v)$; we are thus "in compliance." (For the damped example of Section 4 we suitably complexify our field variable and space and replace $E_{ijk\ell}$ with a very simple "hysteretic" Kelvin model [4] $E_{ijk\ell}(1 + \sqrt{-1} d_m)$; here d_m is a material damping constant.)

We now map $\Omega^o(z, L)$ via a continuous piecewise-affine transformation to a fixed domain Ω. This new problem can now be cast precisely in the desired abstract form of Section 2, in which Ω, X, and (w, v) are independent of the parameter μ: as required, all parameter dependence now enters through the bilinear and linear forms. Furthermore, it is readily demonstrated that our affine assumption applies for $Q = 10$; the $\Theta^q(\mu)$ are of the form $\mu^{y_1}_{(1)} \mu^{y_2}_{(2)} \mu^{y_3}_{(3)}$ for exponents $y_1 = 0$ or 1, $y_2 = -1, 0$, or 1, and $y_3 = -1, 0$, or 1. See [21] for detail of the $\Theta^q(\mu)$, $a^q(w, v)$, $1 \le q \le Q$,

and the "bound conditioner" $(\cdot,\cdot)$.

We shall consider two different models. In Model I, relevant to the Assess stage, we consider the parameter domain $\mathcal{D}^{\rm I} \equiv [3.2, 4.8] \times \mathcal{D}^{z,L}$, where $\mathcal{D}^{z,L} \equiv [0.9, 1.1] \times [0.15, 0.25]$. Note that $\mathcal{D}^{\rm I}$ does not contain any resonances, and hence $\beta(\mu)$ is bounded away from zero; however, $\omega^2 = 3.2$ and $\omega^2 = 4.8$ are quite close to corresponding natural frequencies, and hence the problem is distinctly non-coercive. In Model II, relevant to the Act stage, we consider the parameter domain $\mathcal{D}^{\rm II} \equiv [\omega^2 = 0] \times \mathcal{D}^{z,L}$, where — as in Model I — $\mathcal{D}^{z,L} \equiv [0.9, 1.1] \times [0.15, 0.25]$. Note that Model II is essentially steady linear elasticity and thus the problem is coercive and relatively easy; we shall hence focus our attention on Model I.

We first present basic numerical results. For our reduced-basis spaces we pursue the optimal sampling strategy described in Section 4 for $N^{\rm I}_{\rm max} = 32$ (Model I) and $N^{\rm II}_{\rm max} = 6$ (Model II); for our inf-sup lower bound samples we choose $\bar{\epsilon} = 1/5$ which yields $J^{\rm I} = 84$ and $J^{\rm II} = 1$. We present in Table 1 $\Delta_{N,\rm max,rel}$, $\eta_{N,\rm ave}$, $\Delta^s_{N,\rm max}$, and $\eta^s_{N,\rm ave}$ as a function of $N = N^{\rm I}$ for Model I. Here $\Delta_{N,\rm max,rel}$ is the maximum over $\Xi_{\rm Test}$ of $\Delta_N(\mu)/\|u_{N_{\rm max}}(\mu)\|_{\rm max}$, $\eta_{N,\rm ave}$ is the average over $\Xi_{\rm Test}$ of $\Delta_N(\mu)/\|u(\mu) - u_N(\mu)\|$, $\Delta^s_{N,\rm max,rel}$ is the maximum over $\Xi_{\rm Test}$ of $\Delta^s_N(\mu)/|s_{N_{\rm max}}(\mu)|_{\rm max}$, and $\eta^s_{N,\rm ave}$ is the average over $\Xi_{\rm Test}$ of $\Delta^s_N(\mu)/|s(\mu) - s_N(\mu)|$. Here $\Xi_{\rm Test} \in (\mathcal{D}^{\rm I})^{343}$ is a random parameter sample of size 343, $\|u_{N_{\rm max}}(\mu)\|_{\rm max} \equiv \max_{\mu\in\Xi_{\rm Test}} \|u_{N_{\rm max}}(\mu)\| = 2.0775$, and $|s_{N_{\rm max}}(\mu)|_{\rm max} \equiv \max_{\mu\in\Xi_{\rm Test}} |s_{N_{\rm max}}(\mu)| = 0.089966$. We observe that the RB approximation converges very rapidly, and that our rigorous error bounds are in fact quite sharp. The effectivities are not quite $O(1)$ primarily due to the relatively crude inf-sup lower bound. (Thanks to the rapid convergence of RB approximations, $O(10)$ effectivities do not significantly (adversely) affect efficiency.)

N	$\Delta_{N,\rm max,rel}$	$\eta_{N,\rm ave}$	$\Delta^s_{N,\rm max,rel}$	$\eta^s_{N,\rm ave}$
10	6.19E-01	13.11	8.40E-01	22.50
15	5.76E-02	13.44	4.74E-03	17.22
20	1.58E-02	13.22	4.50E-04	15.44
25	5.69E-03	12.57	4.47E-05	14.50
30	1.32E-03	12.47	2.95E-06	14.27

Table 1: Numerical results for Model I.

Turning now to computational effort (again for Model I), for $N = N^{\rm I} = 25$ and any given μ (say, $4.0, 1.0, 0.2$) — for which the error in the reduced-basis output $s_N(\mu)$ relative to the truth (approximation) $s(\mu)$ is *certifiably* less than $\Delta^s_N(\mu)$ (say, 2.38×10^{-7}) — the Online Time to compute both $s_N(\mu)$ and $\Delta^s_N(\mu)$ is less than 1/330 times the Time to directly calculate $s(\mu) = \ell(u(\mu))$. Clearly, the savings will be even larger for problems with more complex geometry and solution structure in particular in three space dimensions. Nevertheless, even for our current very modest example, the computational economies are very significant.

We now consider an Assess-Act scenario that illustrates the new capabilities enabled by rapid certified input-output evaluation [1]. We first consider the Assess stage (based on Model I): given experimental measurements in the form of intervals $[s(\omega_k^2, z^*, L^*)(1-\epsilon_{\rm exp}),\ s(\omega_k^2, z^*, L^*)(1+\epsilon_{\rm exp})]$, $1 \le k \le K$, we wish to determine a region $\mathcal{R} \in \mathcal{D}^{z,L}$ in which the true but unknown crack parameters, $(z^*,\ L^*)$, must reside. We first introduce $s^{\pm}_N(\mu) \equiv s_N(\mu) \pm \Delta^s_N(\mu)$, and recall that — thanks to our bound theorem (2) — $s(\mu) \in [s^-_N(\mu), s^+_N(\mu)]$. We may then define

$$\mathcal{R} \equiv \big\{(z,L) \in \mathcal{D}^{z,L} \,|\, [s^-_N(\omega_k^2, z, L), s^+_N(\omega_k^2, z, L)] \cap [s(\omega_k^2, z^*, L^*)(1-\epsilon_{\rm exp}), s(\omega_k^2, z^*, L^*)(1+\epsilon_{\rm exp})] \neq \emptyset, 1 \le k \le K\big\};$$

clearly, we have accommodated both *numerical* and *experimental* error and uncertainty (within our model assumptions), and hence $(z^*, L^*) \in \mathcal{R}$.

In Figure 1(b) we present $\mathcal{R}$ for $K = 2$ and $(\omega_1^2 = 3.2,\ \omega_2^2 = 4.8)$ for $\epsilon_{\text{exp}} = 0.5\%, 1\%, 5\%$. (In actual practice, we first find one point in $\mathcal{R}$; we then conduct a binary chop at different angles to map out the boundary of $\mathcal{R}$.) As expected, as ϵ_{exp} decreases, $\mathcal{R}$ shrinks towards the exact (synthetic) value, $z^* = 1.05, L^* = 0.17$. More importantly, for any finite ϵ_{exp}, $\mathcal{R}$ *rigorously captures the uncertainty* in our assessment of the crack parameters without *a priori* regularization hypotheses [7]. The crucial new ingredient is reliable fast evaluations that permit us to conduct a much more extensive search over parameter space; for a given ϵ_{exp}, $\mathcal{R}$ may be generated online in less than 51 seconds on a Pentium 1.6 GHz laptop. Our search over possible crack parameters will certainly never be truly exhaustive, and hence there may be small undiscovered "pockets of possibility" in $\mathcal{D}^{z,L}$; however, we have clearly reduced the uncertainty relative to more conventional approaches. (Of course, our procedure can also only *characterize* cracks within the specified low-dimensional parametrization; however, more general null hypotheses can be constructed to *detect* model deviation.)

Finally, we consider the Act stage (based on Model II). We presume here that the component must withstand an in-service steady force (normalized to unity) such that the deflection $s(0, z^*, L^*)$ in the "next mission" does not exceed a specified value $s_{\max}$. Of course, in practice, we will not be privy to (z^*, L^*). To address this difficulty we first define $s_{\mathcal{R}}^+ = \max_{(z,L)\in\mathcal{R}} s_N^+(0, z, L)$, where $s_N^+(0, z, L) = s_N(0, z, L) + \Delta_N^s(0, z, L)$; our corresponding "go/no-go" criterion is then given by $s_{\mathcal{R}}^+ \le s_{\max}$. It is readily observed that $s_{\mathcal{R}}^+$ rigorously accommodates both experimental (crack) and numerical uncertainty — $s(0, z^*, L^*) \le s_{\mathcal{R}}^+$ — and that the associated go/no-go discriminator is hence *fail-safe*. Furthermore, as ϵ_{exp} tends to zero and N^{I} and N^{II} increase, $s_{\mathcal{R}}^+$ will tend to $s(0, z^*, L^*)$; indeed, for $\epsilon_{\text{exp}} = 1\%$ and $N^{\text{I}} = 25$, $N^{\text{II}} = 6$, $[s_{\mathcal{R}}^+ - s(0, z^*, L^*)]/|s(0, z^*, L^*)| = 4.73\text{E-}05$. In summary, in real-time, we can both Assess the current state of the crack and subsequently Act to ensure the safety (or optimality) of the next "sortie."

6 Incompressible Navier-Stokes Equations

To illustrate the difficulties that arise in the treatment of nonlinear problems we consider a particular example [34]: the steady incompressible Navier-Stokes equations — Pr(andtl) = 0 natural convection in an enclosure [29, 32].

Our formulation of Section 2 is still applicable (except a is no longer bilinear): $\mu \equiv \text{Gr} \equiv$ Grashof number; $\mathcal{D} \equiv [1.0, 1.0\text{E}5]$; $u^{\text{e}}(\mu) = (u_1^{\text{e}}(\mu), u_2^{\text{e}}(\mu))$ is the velocity field; $\Omega = [0, 4] \times [0, 1]$; $X^{\text{e}} = \{(H_0^1(\Omega))^2 \,|\, \nabla\cdot v = 0\}$; $(w, v) = \int_\Omega w_{i,j} v_{i,j}$; $a(w, v) = a_0(w, v) + \frac{1}{2} a_1(w, w, v)$, where $a_0(w, v) \equiv \int_\Omega w_{i,j} v_{i,j}$ and $a_1(w, z, v) \equiv -\int_\Omega (w_i z_j + w_j z_i) v_{i,j}$ are the viscous and convective terms, respectively; $f(v; \mu) = \mu f_0(v) = \mu \int_\Omega \left(1 - \frac{1}{4} x_1\right) v_2$ is the buoyancy contribution; and $\ell(v) \equiv 2 \int_{\Gamma_0} v_1(x) dx_2$ (for $\Gamma_0 = \{x_1 = 2, x_2 \in [0.5; 1]\}$) measures the flowrate. (Note that the pressure does not appear explicitly since we pose the problem over divergence-free velocity fields.)

We next introduce X, a reference finite element approximation space. Our reference (or "truth") finite element approximation $u(\mu) \in X$ is then defined by $a(u(\mu), v) = f(v; \mu)$, $\forall\, v \in X$. As before, $u(\mu)$ is a surrogate for $u^{\text{e}}(\mu)$ upon which we build our RB approximation, and relative to which we measure our RB error. Here X is the space (of dimension $\mathcal{N} = 2{,}786$) of discretely divergence-free functions associated with a classical Taylor-Hood $\mathbb{P}_2 - \mathbb{P}_1$ finite element approximation [9]. (For future reference, we also define $\widetilde{X}$, the full Taylor-Hood velocity space.)

The derivative of a plays a central role: here $da(w, v; z) \equiv a_0(w, v) + a_1(w, z, v)$ satisfies $a(z + w, v) = a(z, v) + da(w, v; z) + \frac{1}{2} a_1(w, w, v)$. It is readily shown [34] that $da(w, v; z) \le \gamma(z) \|w\| \|v\|$ for $\gamma(z) = 1 + \rho^2 \|z\|$; here $\rho \equiv \sqrt{2} \sup_{v\in\widetilde{X}} \|v\|_{L^4(\Omega)} / \|v\|$ is a Sobolev embedding

constant [33], and $\|v\|_{L^p(\Omega)} \equiv (\int_\Omega (w_i w_i)^{p/2})^{1/p}$. We shall further assume [34] — and verify *a posteriori* — that $\{u(\mu) \,|\, \mu \in \mathcal{D}\}$ is a nonsingular (isolated) solution branch: $\beta(u(\mu)) \geq \beta_0 > 0, \forall\, \mu \in \mathcal{D}$, where $\beta(z) \equiv \inf_{w\in X} \sup_{v\in X} da(w, v; z)/\|w\|\|v\|$ is the inf-sup parameter relevant to our nonlinear problem. Numerical simulations [29, 32] demonstrate that the flow *smoothly evolves* from a single-cell structure for the lower Gr in $\mathcal{D}$ to an inertia-dominated three-cell structure for the higher Gr in $\mathcal{D}$.

We may directly apply the RB formulation of Section 3 to the incompressible Navier-Stokes equations [12, 24, 34]. The most significant new issue is (efficient) calculation of the nonlinear terms. We consider the inner Newton update: given a current iterate $\overline{u}_N(\mu) = \sum_{n=1}^N \overline{u}_{N\,n}(\mu)\,\zeta_n$, we must find an increment $\delta u_N \in W_N$ such that $da(\delta u_N, v; \overline{u}_N) = R(v;\mu)$, $\forall\, v \in W_N$; here $R(v;\mu) \equiv f(v;\mu) - a(u_N(\mu), v)$, $\forall\, v \in X$ is the residual. The associated algebraic equations are thus

$$\sum_{j=1}^N \Big\{a_0(\zeta_j,\zeta_i) + \sum_{n=1}^N \overline{u}_{N\,n}(\mu) a_1(\zeta_j,\zeta_n,\zeta_i)\Big\}\delta u_{N\,j} = \mu f_0(\zeta_i) - \sum_{j=1}^N \Big\{a_0(\zeta_j,\zeta_i) + \tfrac{1}{2}\sum_{n=1}^N \overline{u}_{N\,n}(\mu) a_1(\zeta_j,\zeta_n,\zeta_i)\Big\}\overline{u}_{N\,j}(\mu),\ \forall\, i \in \mathbb{N},$$

where we recall that $f(v;\mu) = \mu f_0(v)$ and $\mu \equiv \mathrm{Gr}$.

We can directly apply the offline-online procedure described in Section 3 for linear problems, except now we must perform summations both over the affine parameter dependence (rather trivial here) *and* over the reduced-basis coefficients (of the current Newton iterate, $\overline{u}_N(\mu)$). In the online stage — for given new μ — at each Newton iteration $\overline{u}_N(\mu) \rightarrow \delta u_N$ we first assemble the right-hand side (residual) — at cost $O(N^3)$; we then form and invert the left-hand side (Jacobian) — at cost $O(N^3)$. The complexity of the online stage is independent of $\mathcal{N}$: furthermore, for our quadratic nonlinearity, there is little increased cost relative to the linear case. Unfortunately, for a p^{th}-order nonlinearity, the online cost for the residual assembly and Jacobian formation will scale as $O(N^{p+1})$, and thus standard Galerkin projections are viable only for $p = 2$ or at most $p = 3$ [36]. Fortunately, for larger p and non-polynomial nonlinearities — and for non-affine parameter dependence [5] — quite effective collocation-like alternatives are available.

Turning now to *a posteriori* error estimation, we first "presume" $\tilde{\beta}_N(\mu)$, a (to-be-constructed) positive lower bound for the inf-sup parameter $\beta_N(\mu) \equiv \beta(u_N(\mu))$: $\beta_N(\mu) \geq \tilde{\beta}_N(\mu) \geq 0$, $\forall\, \mu \in \mathcal{D}$. We next recall the dual norm of the residual, $\varepsilon_N(\mu) \equiv \sup_{v\in X} R(v;\mu)/\|v\|$, and introduce $\tau_N(\mu) \equiv 2\rho^2 \varepsilon_N(\mu)/\tilde{\beta}_N^2(\mu)$, where ρ is our $L^4(\Omega)$-$\widetilde{X}$ embedding constant. Finally, we define $N^*(\mu)$ such that $\tau_N(\mu) < 1$ for $N \geq N^*(\mu)$; we require $N^*(\mu) \leq N_{\max}$, $\forall\, \mu \in \mathcal{D}$. (The latter is a condition on $N_{\max}$ that reflects both the convergence rate of the RB approximation and the quality of our inf-sup lower bound.)

We may now define our error estimator: for $N \geq N^*(\mu)$, $\Delta_N(\mu) \equiv (\tilde{\beta}_N(\mu)/\rho^2)(1 - \sqrt{1 - \tau_N(\mu)})$; note that, as $\varepsilon_N(\mu) \rightarrow 0$, $\Delta_N(\mu)$ tends to the "linear case" $\varepsilon_N(\mu)/\tilde{\beta}_N(\mu)$. Our main result is then: given any $\mu \in \mathcal{D}$, for all $N \geq N^*(\mu)$, there exists a unique (truth approximation) solution $u(\mu) \in X$ in the ball $\mathcal{B}(u_N(\mu), \tilde{\beta}_N(\mu)/\rho^2) \equiv \{z \in X \,|\, \|z - u_N(\mu)\| < \tilde{\beta}_N(\mu)/\rho^2\}$; furthermore, $\|u(\mu) - u_N(\mu)\| \leq \Delta_N(\mu)$. The proof [34, 35] is a slight specialization of the abstract "Brezzi-Rappaz-Raviart" result [6, 11]; we can further provide several corollaries related to (*i*) the well-posedness of the truth approximation, and (*ii*) the effectivity of our error bound [34]. (We may also develop bounds for the output of interest [34].)

The real challenge, is computational: how can we compute $\varepsilon_N(\mu)$, ρ, and $\tilde{\beta}_N(\mu)$? (Note that, armed with these quantities, we can evaluate $\tau_N(\mu)$ and hence verify $N \geq N^*(\mu)$.) The reduced-basis context is in fact a rare opportunity to render the Brezzi-Rappaz-Raviart theory *completely*

quantitative. To begin, we consider $\varepsilon_N(\mu)$: as for the linear case, we invoke duality, our reduced-basis expansion, the affine parameter dependence of a (and f), and linear superposition to express

$$\varepsilon_N^2(\mu) = \mu^2(\mathcal{C},\mathcal{C}) + \sum_{n=1}^{N} u_{N\,n}(\mu)\left\{2\mu(\mathcal{C},\mathcal{L}_n) + \sum_{n'=1}^{N} u_{N\,n'}(\mu)\left\{2\mu(\mathcal{C},\mathcal{Q}_{n\,n'}) + (\mathcal{L}_n,\mathcal{L}_{n'})\right.\right.$$
$$\left.\left. + \sum_{n''=1}^{N} u_{N\,n''}(\mu)\left\{2(\mathcal{L}_n,\mathcal{Q}_{n'n''}) + \sum_{n'''=1}^{N} u_{N\,n'''}(\mu)\,(\mathcal{Q}_{n\,n'},\mathcal{Q}_{n''n'''})\right\}\right\}\right\}, \quad (4)$$

where $(\mathcal{C},v) = f(v)$, $\forall\, v \in X$, $(\mathcal{L}_n,v) = -a_0(\zeta_n,v)$, $\forall\, v \in X$, $\forall\, n \in \mathbb{N}$, and $(\mathcal{Q}_{n\,n'},v) = -\frac{1}{2}a_1(\zeta_n,\zeta_{n'},v)$, $\forall\, v \in X$, $\forall\,(n,n') \in \mathbb{N}^2$; the latter are again simple (vector) Poisson problems.

We can now readily adapt the offline-online procedure developed in the linear case [34, 35]. In the online stage — for each new μ — we perform the sum (4) in terms of the *pre*-formed and *stored* inner products (for example, $(\mathcal{Q}_{nn'},\mathcal{Q}_{n''n'''}), 1 \le n,n',n'',n''' \le N$) and the RB coefficients $u_{N\,n}(\mu)$, $1 \le n \le N$ — at cost $O(N^4)$. Although the N^4 scaling, which arises due to the trilinear term in the residual, is certainly unpleasant, the error bound is calculated only once: in actual practice, the additional online cost attributable to the dual norm of the residual is not too large. Unfortunately, for a p^{th}-order nonlinearity, the online evaluation of $\varepsilon_N(\mu)$ scales as $O(N^{2p})$, and our approach is thus viable only for $p = 2$. Fortunately, for larger p and non-polynomial nonlinearities — and for non-affine parameter dependence [5] — collocation-like alternatives are available; however, in general, there will be some *loss of rigor.*

We next turn to the calculation of ρ. The critical observation is that ρ is the supremum of a "Rayleigh-quotient." Thus ρ is related to the smallest multiplier of an associated Euler-Lagrange nonlinear eigenproblem [33]: $(\hat{\lambda},\hat{\psi}) \in (\mathbb{R}_+,\widetilde{X})$ satisfies $(\hat{\psi},v) = 2\hat{\lambda}^2\int_\Omega \hat{\psi}_j\hat{\psi}_j\hat{\psi}_i v_i$, $\forall\, v \in \widetilde{X}$, for $\|\hat{\psi}\|^4_{L^4(\Omega)} = 1$; the ground state is denoted $(\hat{\lambda}_{\min},\hat{\psi}_{\min})$, and $\rho = \hat{\lambda}_{\min}^{-1}$. In practice, it may be difficult to isolate the ground state; we thus consider a homotopy procedure.

Towards that end, we first introduce a parametrized generalization of the Euler-Lagrange equation: given $\alpha \in [0,1]$, $(\lambda(\alpha),\psi(\alpha)) \in (\mathbb{R}_+,\widetilde{X})$ satisfies $(\psi,v) = 2\lambda^2(\alpha)[\alpha\int_\Omega \psi_j(\alpha)\psi_j(\alpha)\psi_i(\alpha)v_i + (1-\alpha)\int_\Omega \psi_i(\alpha)v_i]$, $\forall\, v \in \widetilde{X}$, for normalization $\alpha\|\psi(\alpha)\|^4_{L^4} + (1-\alpha)\|\psi(\alpha)\|^2_{L^2} = 1$; the ground state is denoted $(\lambda_{\min}(\alpha),\psi_{\min}(\alpha))$, and $\rho = \lambda_{\min}^{-1}(1)$. We may now apply standard Newton continuation methods to proceed from the known ground state at $\alpha = 0$ — $(\lambda_{\min}(0),\psi_{\min}(0))$ is the lowest eigenpair of a simple (vector) "Laplacian" linear eigenproblem — to the ground state of interest at $\alpha = 1$; for sufficiently small increments in α, we will remain on the desired (lowest-energy) branch. For our particular domain, we find (offline) $\rho = 0.4416$; since ρ is μ-independent, no online computation is required.

Finally, as regards the inf-sup lower bound, $\tilde{\beta}_N(\mu)$, we may directly apply appropriate extensions [21, 34] of the procedure developed in Section 5. The nonlinear case does present a new difficulty: the parameter dependence of the (linearized) operator is now induced by the reduced-basis solution $u_N(\mu)$ — in our case, through the $a_1(w,u_N(\mu),v)$ term — and hence is *not known a priori.* Fortunately, since $u_N(\mu) \to u(\mu)$ we may develop a "universal" lower bound for sufficiently large N; the complications are thus largely practical in nature. (For our particular problem, $J = 34$ — the sample is relatively small despite the rather large range in Grashof.)

We conclude with a brief discussion of the adaptive sampling procedure introduced in Section 4. In the nonlinear case a similar procedure may be pursued, but with two important differences. First, as already indicated, $\beta_N(\mu)$ and hence $\tilde{\beta}_N(\mu)$ will now depend on the reduced-basis solution $u_N(\mu)$; furthermore, $\beta_N(\mu)$ will only be meaningful for larger N. Thus in the sample construction stage we must replace $\tilde{\beta}_N(\mu)$ in $\Delta_N(\mu)$ with a simple but relevant surrogate — for example, a piecewise-constant (over $\mathcal{D}$) approximation to $\beta(u(\mu))$. Second, in the nonlinear context our error

	Gr = 1.0E1			Gr = 8.5E4		
N	τ_N	$\Delta_{N,\text{rel}}$	η_N	τ_N	$\Delta_{N,\text{rel}}$	η_N
3	2.0 E−2	5.0 E−2	1.0	∞	*	*
6	1.2 E−2	3.0 E−2	1.0	2.8 E+1	*	*
9	4.4 E−3	1.1 E−2	1.0	5.2 E−1	1.5 E−4	14.1
12	2.7 E−6	6.8 E−6	1.0	5.8 E−1	1.7 E−4	20.5
15	3.0 E−7	7.6 E−7	1.0	1.9 E−2	4.6 E−6	17.6

Table 2: Error bounds and effectivities for Gr = 1.0E1 and Gr = 8.5E4.

bound is conditional — a small solution to the error equation is only assured if $\tau_N(\mu) < 1$. Thus the greedy procedure must first select on $\arg\max_{\mu\in\Xi^F} \tau_N(\mu)$ — until $\tau_N(\mu) < 1$, $\forall\, \mu \in \Xi^F$ — and only subsequently select on $\arg\max_{\mu\in\Xi^F} \Delta_N(\mu)$; the resulting sample will ensure rapid convergence to a *certifiably* accurate solution.

In Table 2 we present $\Delta_{N,\text{rel}}(\mu) \equiv \Delta_N(\mu)/\|u_{N_{\max}}(\mu)\|$ and $\eta_N(\mu) \equiv \Delta_N(\mu)/\|u(\mu) - u_N(\mu)\|$ as a function of N for $\mu = \text{Gr} = 1.0\text{E}1$ (single-roll) and $\mu = \text{Gr} = 8.5\text{E}4$ (three-roll). The "*" indicates that $N < N^*(\mu)$ — $\tau_N(\mu) \geq 1$: no error bound is available. For Gr = 1.0E1, we find $N^*(\mu) = 1$, and hence we obtain error bounds for all N; the error bound tends to zero very rapidly; and the effectivity is $O(1)$ [21, 34]. For Gr = 8.5E4, we find $N^*(\mu) = 9$, and hence we obtain error bounds only for rather accurate approximations; however, the error bound still tends to zero rapidly with N — our samples S_N^{opt} are constructed to provide uniform convergence; and the effectivity is still quite good. It is perhaps surprising that the Brezzi-Rappaz-Raviart theory — not really designed for quantitative service — indeed yields such sharp results; in fact, as $\varepsilon_N(\mu) \to 0$, the cruder bounds — in particular, ρ — no longer play a role.

Finally, we note that the online cost (on a Pentium® M 1.6GHz processor) to predict $s_N(\mu)$ and $\Delta_N(\mu)$ (and a bound for the error in the output, $\Delta_N^s(\mu)$ [34]) is typically 10ms and 90ms, respectively — compared to order minutes for direct finite element calculation of $s(\mu) = \ell(u(\mu))$.

7 Parabolic Equations

We consider here the extension of the RB methods and associated *a posteriori* error estimators described in Sections 1-4 to *parabolic* PDEs — in particular, the heat equation; we shall "simply" treat time as an additional, albeit special, parameter [30]. (There are many approaches to model reduction for initial-value problems: POD methods [31]; balanced-truncation techniques [20]; and even reduced-basis approaches [26]. However, in general, these frameworks do not accommodate parametric variation (or, typically, rigorous *a posteriori* error estimation).) For simplicity, we directly consider a K-level time-discrete framework (corresponding to Euler Backward discretization — we can also readily treat higher-order schemes such as Crank-Nicolson) associated to the time interval $[0, t_f]$: we define $\mathbb{T} \equiv \{t^0, \ldots, t^K\}$, where $t^k = k\Delta t$, $0 \leq k \leq K$, and $\Delta t = t_f/K$; for notational convenience, we also introduce $\mathbb{K} = \{1, \ldots, K\}$. (Clearly, our results must be stable as $\Delta t \to 0$, $K \to \infty$.)

Given $\mu \in \mathcal{D} \subset \mathbb{R}^P$, we evaluate the (here, single) output $s(\mu, t^k) = \ell(u(\mu, t^k))$, $\forall\, k \in \mathbb{K}$, where $u(\mu, t^k) \in X$, $\forall\, k \in \mathbb{K}$, satisfies

$$\Delta t^{-1} m(u(\mu, t^k) - u(\mu, t^{k-1}), v) + a(u(\mu, t^k), v; \mu) = b(t^k) f(v), \quad \forall\, v \in X, \tag{5}$$

with initial condition (say) $u(\mu, t^0) = 0$. Here μ and $\mathcal{D}$ are the input and input domain; $u(\mu, t^k)$, $\forall\, k \in \mathbb{K}$, is our field variable; $X \subset X^{\text{e}}$ is our truth approximation subspace for X^{e} (and $(\cdot,\cdot)$, $\|\cdot\|$) defined in Section 2; $a(\cdot,\cdot;\mu)$ and $m(\cdot,\cdot)$ are X^{e}-continuous and $L^2(\Omega)$-continuous symmetric

bilinear forms, respectively; $f(\cdot)$, $\ell(\cdot)$ are $L^2(\Omega)$-continuous linear forms; and $b(t^k)$ is the (here, single) "control" input at time t^k.

We shall make the following assumptions. First, we require that a and m are independent of time — the system is thus linear time-invariant (LTI). Second, we assume that a and m are coercive: $0 < \alpha_0 \leq \alpha(\mu) \equiv \inf_{v\in X}[a(v,v;\mu)/\|v\|^2]$ and $0 < \sigma_0 \leq \sigma(\mu) \equiv \inf_{v\in L^2(\Omega)}[m(v,v)/\|v\|^2_{L^2(\Omega)}]$. Third, we assume that a depends affinely on μ: $a(w,v;\mu) = \sum_{q=1}^{Q} \Theta^q(\mu)\, a^q(w,v)$ for $q = 1,\ldots,Q$ parameter-*dependent* functions $\Theta^q(\mu) : \mathcal{D} \to \mathbb{R}$ and parameter-*independent* continuous bilinear forms $a^q(w,v)$. (For simplicity, we assume that m, f, and ℓ are parameter-independent.)

To ensure rapid convergence of the reduced-basis output approximation we shall need a dual (or adjoint) problem which shall evolve backward in time. Invoking the LTI property, we can express the adjoint for the output at time t^L, $1 \leq L \leq K$, as $\psi^L(\mu,t^k) \equiv \Psi(\mu,t^{K-L+k})$, $1 \leq k \leq L$; here $\Psi(\mu,t^k) \in X$, $\forall\, k \in \mathbb{K}$, satisfies $\Delta t^{-1} m(v,\Psi(\mu,t^k) - \Psi(\mu,t^{k+1})) + a(v,\Psi(\mu,t^k);\mu) = 0$, $\forall\, v \in X$, with final condition $m(v,\Psi(\mu,t^{K+1})) \equiv \ell(v)$, $\forall\, v \in X$.

We now introduce the nested samples $S^{\rm pr}_{N_{\rm pr}} = \{\tilde\mu^{\rm pr}_1,\ldots,\tilde\mu^{\rm pr}_{N_{\rm pr}}\}$, $1 \leq N_{\rm pr} \leq N_{\rm pr,max}$, and $S^{\rm du}_{N_{\rm du}} = \{\tilde\mu^{\rm du}_1,\ldots,\tilde\mu^{\rm du}_{N_{\rm du}}\}$, $1 \leq N_{\rm du} \leq N_{\rm du,max}$, where $\tilde\mu \equiv (\mu,t^k) \subset \widetilde{\mathcal{D}} \equiv \mathcal{D}\times\mathbb{T}$. Note the samples must now reside in the *parameter-time* space $\widetilde{D}$; we also introduce separate (and different) samples for the primal and dual problems. We then define the associated nested RB spaces $W^{\rm pr}_{N_{\rm pr}} = {\rm span}\{\zeta^{\rm pr}_n \equiv u(\tilde\mu^{\rm pr}_n = (\mu_n,t^{k_n})^{\rm pr}),\ 1 \leq n \leq N_{\rm pr}\}$, $1 \leq N_{\rm pr} \leq N_{\rm pr,max}$, and $W^{\rm du}_{N_{\rm du}} = {\rm span}\{\zeta^{\rm du}_n \equiv \psi(\tilde\mu^{\rm du}_n = (\mu_n,t^{k_n})^{\rm du}),\ 1 \leq n \leq N_{\rm du}\}$, $1 \leq N_{\rm du} \leq N_{\rm du,max}$. Note that for the primal basis we choose — as justified by the LTI hypothesis — an impulse input, $b(t^k) = \delta_{1k}$, $\forall\, k \in \mathbb{K}$.

Our RB approximation is then: given $\mu \in \mathcal{D}$, evaluate $s_N(\mu,t^k) = \ell(u_N(\mu,t^k)) + \sum_{k'=1}^{k} R^{\rm pr}(\Psi_N(\mu,t^{K-k+k'});\mu,t^{k'})\ \Delta t$, $\forall\, k \in \mathbb{K}$, where (pr) $u_N(\mu,t^k) \in W^{\rm pr}_{N_{\rm pr}}$, $\forall\, k \in \mathbb{K}$, satisfies $\Delta t^{-1} m(u_N(\mu,t^k) - u_N(\mu,t^{k-1}),v) + a(u_N(\mu,t^k),v;\mu) = b(t^k)\ f(v)$, $\forall\, v \in W^{\rm pr}_{N_{\rm pr}}$, with initial condition $u_N(\mu,t^0) = 0$, and (du) $\Psi_N(\mu,t^k) \in W^{\rm du}_{N_{\rm du}}$, $\forall\, k \in \mathbb{K}$, satisfies $\Delta t^{-1} m(v,\Psi_N(\mu,t^k) - \Psi_N(\mu,t^{k+1})) + a(v,\Psi_N(\mu,t^k);\mu) = 0$, $\forall\, v \in W^{\rm du}_{N_{\rm du}}$, with final condition $m(v,\Psi_N(\mu,t^{K+1})) \equiv \ell(v)$, $\forall\, v \in W^{\rm du}_{N_{\rm du}}$. Here, $\forall\, k \in \mathbb{K}$, $R^{\rm pr}(v;\mu,t^k) \equiv b(t^k)\ f(v) - (\Delta t^{-1} m(u_N(\mu,t^k) - u_N(\mu,t^{k-1}),v) + a(u_N(\mu,t^k),v;\mu))$, $\forall\, v \in X$, is the primal residual.

The offline-online computational procedure is similar to the elliptic case of Section 3 but with the added complexity of the dual problem and the time dependence. In the *online* stage, we first assemble the requisite RB "stiffness" matrices — at cost $O((N^2_{\rm pr}+N^2_{\rm du}+N_{\rm pr}N_{\rm du})Q)$; we then solve the primal and dual problems — at cost $O(N^3_{\rm pr}+N^3_{\rm du}+K(N^2_{\rm pr}+N^2_{\rm du}))$; and finally we evaluate the RB output approximation $s_N(\mu;t^k)$, $\forall\, k \in \mathbb{K}$ — at cost $O(KN_{\rm pr}N_{\rm du})$. The online complexity is thus *independent* of $\mathcal{N}$, and in fact not too sensitive (for our LTI system) to K.

We now turn to *a posteriori* error estimation. We stress that the development of the error bounds is in no way limited to the RB approximation described here: we may consider "any" stable ODE or PDE system and any reduced-order model. To begin, we assume that we are given $\tilde\alpha(\mu) : \mathcal{D} \to \mathbb{R}_+$ — a positive lower bound for the coercivity constant, $\alpha(\mu)$: $\alpha(\mu) \geq \tilde\alpha(\mu) \geq \tilde\alpha_0 > 0$, $\forall \mu \in \mathcal{D}$. In our symmetric case $\alpha(\mu) = \beta(\mu)$ and thus $\tilde\alpha(\mu)$ can be constructed according to Section 4; in fact, thanks to coercivity, much simpler procedures typically suffice [27]. We next recall the dual norm of the primal and dual residuals: $\forall\, k \in \mathbb{K}$, $\varepsilon^{\rm pr}_{N_{\rm pr}}(\mu,t^k) \equiv \sup_{v\in X}[R^{\rm pr}(v;\mu,t^k)/\|v\|]$ and $\varepsilon^{\rm du}_{N_{\rm du}}(\mu,t^k) \equiv \sup_{v\in X}[R^{\rm du}(v;\mu,t^k)/\|v\|]$, where $\forall\, k \in \mathbb{K}$, $R^{\rm du}(v;\mu,t^k) \equiv -(\Delta t^{-1} m(v,\Psi_N(\mu,t^k) - \Psi_N(\mu,t^{k+1})) + a(v,\Psi_N(\mu,t^k);\mu))$, $\forall\, v \in X$. Finally, we introduce the "spatio-temporal" energy norm, $|||v(\mu,t^k)|||^2 \equiv m(v(\mu,t^k),v(\mu,t^k)) + \sum_{k'=1}^{k} \Delta t\ a(v(\mu,t^{k'}),v(\mu,t^{k'});\mu)$, $\forall\, v \in X$.

We may now define our error estimators: $\forall\, k \in \mathbb{K}$, $\forall\, \mu \in \mathcal{D}$, $\Delta^{\rm pr}_{N_{\rm pr}}(\mu,t^k) \equiv \tilde\alpha^{-\frac{1}{2}}(\mu)\big(\Delta t \sum_{k'=1}^{k}$

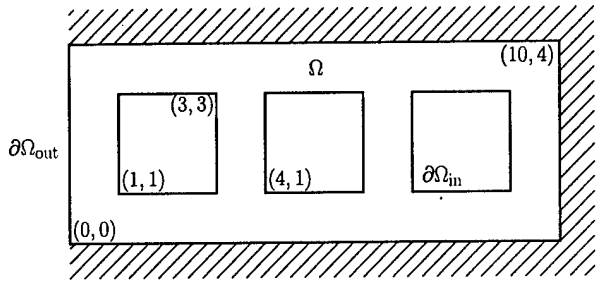

Figure 2: One "cell" of the heat shield.

$\varepsilon^{\text{pr}}_{N_{\text{pr}}}(\mu, t^{k'})^2)^{\frac{1}{2}}$; $\Delta^{\text{du}}_{N_{\text{du}}}(\mu, t^k) \equiv \tilde{\alpha}^{-\frac{1}{2}}(\mu)(\Delta t \sum_{k'=k}^{K} \varepsilon^{\text{du}}_{N_{\text{du}}}(\mu, t^{k'})^2)^{\frac{1}{2}}$; and

$$\Delta^s(\mu, t^k) \equiv \Delta^{\text{pr}}_{N_{\text{pr}}}(\mu, t^k)\ \Delta^{\text{du}}_{N_{\text{du}}}(\mu, t^{K-k+1}). \tag{6}$$

We can then readily demonstrate that $|||u(\mu, t^k) - u_N(\mu, t^k)||| \le \Delta^{\text{pr}}_{N_{\text{pr}}}(\mu, t^k)$ and $|s(\mu, t^k) - s_N(\mu, t^k)| \le \Delta^s(\mu, t^k)$, $\forall\, k \in \mathbb{K}$, $\forall\, \mu \in \mathcal{D}$, $\forall\, N_{\text{pr}} \in \mathbb{N}_{\text{pr,max}}$, $\forall\, N_{\text{du}} \in \mathbb{N}_{\text{du,max}}$ — we obtain rigorous (and, as we shall see, rather sharp) upper bounds for the primal error, dual error, *and* output error. (Note that our particular form (6) assumes that $\Psi(\mu, t^{K+1})$ — here, μ-independent — is a member of $W^{\text{du}}_{N_{\text{du}}}$; this requirement is readily relaxed.)

The offline-online procedure for the computation of $\Delta^s(\mu, t^k)$, $\forall\, k \in \mathbb{K}$ — in particular, for the calculation of the requisite primal and dual residual norms — is similar to the elliptic case of Section 4 but with the added complexity of the dual problem and the time dependence. In particular, in the *online* stage — for any given new μ — we evaluate the $\varepsilon^{\text{pr}}_{N_{\text{pr}}}(\mu, t^k)^2$ and $\varepsilon^{\text{du}}_{N_{\text{du}}}(\mu, t^k)^2$ sums in terms of $\Theta^q(\mu)$, $u_{N\,n}(\mu, t^k)$, $\Psi_{N\,n'}(\mu, t^{k'})$ and the *precomputed* inner products — at cost $O(K(N^2_{\text{pr}} + N^2_{\text{du}})Q^2)$. Thus, all online calculations are indeed *independent* of $\mathcal{N}$.

We now turn to a particular numerical example. We consider the design of a heat shield (one cell of which is shown in Figure 2): the left boundary $\partial\Omega_{\text{out}}$ is exposed to a temperature unity and Biot number Bi_{out} "source" for $t \in [0, t_f]$; the right boundary as well as the top and bottom (symmetry) boundaries are insulated; and the internal boundaries $\partial\Omega_{\text{in}}$ — corresponding to three square cooling channels — are exposed to a temperature zero and Biot number Bi_{in} "sink." Our input parameter is hence $\mu \equiv (\mu_{(1)}, \mu_{(2)}) \equiv (\text{Bi}_{\text{out}}, \text{Bi}_{\text{in}}) \in \mathcal{D} \equiv [0.01, 0.5] \times [0.001, 0.1]$; our output is the average temperature of the structure — a surrogate for the maximum temperature of the (to-be-protected) right boundary for $t \in [0, \infty[$.

The underlying PDE is the heat equation. The (appropriately non-dimensionalized) governing equation for the temperature $u(\mu, t^k) \in X$ is thus (5), where X is a linear finite element truth approximation subspace (of dimension (exploiting symmetry) $\mathcal{N} = 1{,}396$) of $X^{\text{e}} \equiv H^1(\Omega)$; $a(w, v; \mu) \equiv \int_\Omega \nabla w \cdot \nabla v + \mu_{(1)} \int_{\Omega_{\text{out}}} w\, v + \mu_{(2)} \int_{\Omega_{\text{in}}} w\, v$; $m(w, v) \equiv \int_\Omega w\, v$; $f(v; \mu) \equiv \mu_{(1)} \int_{\Omega_{\text{out}}} v$, which is now (affinely) parameter-dependent; $b(t^k) = 1$, $\forall k \in \mathbb{K}$; and $(w, v) \equiv \int_\Omega \nabla w \cdot \nabla v + 0.01 \int_{\partial\Omega_{\text{out}}} w\, v + 0.001 \int_{\partial\Omega_{\text{in}}} w\, v$ — hence we may choose $\tilde{\alpha}(\mu) = 1$. The output is given by $s(\mu, t^k) = \ell(u(\mu, t^k))$, where $\ell(v) \equiv |\Omega|^{-1} \int_\Omega v$.

We now present numerical results. Our "optimal" primal and dual samples are constructed (separately) by procedures similar to the greedy approach described for the elliptic case in Section 4: at each step (say, for the primal) we select the parameter value μ^* for which $\Delta^{\text{pr}}_{N_{\text{pr}}}(\mu, t^K)$ is maximized; we then select the time t^{k^*} for which $\varepsilon^{\text{pr}}_{N_{\text{pr}}}(\mu^*, t^k)$ is maximized. In Table 3 we present, as a function of N_{pr} $(= N_{\text{du}})$, $\Delta^{\text{pr}}_{\text{max,rel}}$, $\overline{\eta}^{\text{pr}}$, $\Delta^s_{\text{max,rel}}$, and $\overline{\eta}^s$: $\Delta^{\text{pr}}_{\text{max,rel}}$ is the maximum over Ξ_{Test} of

$N_{\rm pr}$	$\Delta^{\rm pr}_{\rm max,rel}$	$\overline{\eta}^{\rm pr}$	$\Delta^{s}_{\rm max,rel}$	$\overline{\eta}^{s}$
4	1.6 E−00	5.44	1.6 E−00	95.63
8	6.3 E−02	1.55	6.7 E−03	30.92
12	1.0 E−02	1.03	2.6 E−04	8.43
16	3.2 E−03	1.02	1.5 E−05	11.45
20	8.8 E−04	1.01	1.1 E−06	17.43

Table 3: Convergence results for the heat equation.

$\Delta^{\rm pr}_{N_{\rm pr}}(\mu,t^K)/|||u_N(\mu_u,t^K)|||$, $\overline{\eta}^{\rm pr}$ is the average over $\Xi_{\rm Test}\times\mathbb{T}$ of $\Delta^{\rm pr}_{N_{\rm pr}}(\mu,t^k)/|||u(\mu,t^k)-u_N(\mu,t^k)|||$, $\Delta^{s}_{\rm max,rel}$ is the maximum over $\Xi_{\rm Test}$ of $\Delta^{s}_{N}(\mu,t^K)/|s_N(\mu_s,t^K)|$, and $\overline{\eta}^{s}$ is the average over $\Xi_{\rm Test}$ of $\Delta^{s}_{N}(\mu,t_\eta(\mu))/|s(\mu,t_\eta(\mu))-s_N(\mu,t_\eta(\mu))|$. Here $\Xi_{\rm Test}\in(\mathcal{D})^{400}$ is a random input sample of size 400; $\mu_u \equiv \arg\max_{\mu\in\Xi_{\rm Test}} |||u_{N_{\rm max}}(\mu,t^K)|||$, $\mu_s \equiv \arg\max_{\mu\in\Xi_{\rm Test}} |s_{N_{\rm max}}(\mu,t^K)|$ (note the output grows with time), and $t_\eta(\mu)\equiv \arg\max_{t^k\in\mathbb{T}} |s(\mu,t^k)-s_N(\mu,t^k)|$.

Finally, we note that the calculation of $s_N(\mu,t^k)$ and $\Delta^s_N(\mu,t^k)$, $\forall\, k\in\mathbb{K}$, is (say, for $N_{\rm pr}=N_{\rm du}=12$) roughly 40× faster than direct calculation of the truth approximation output $s(\mu,t^k)=\ell(u(\mu,t^k))$, $\forall\, k\in\mathbb{K}$. We may thus work with $s_N(\mu,t^k)+\Delta^s_N(\mu,t^k)$ as a *certifiably* conservative (upper bound) and accurate surrogate for the average temperature $s(\mu,t^k)$ in truly interactive design exercises.

References

[1] S. Ali. *Real-time Optimal Parametric Design using the Assess-Predict-Optimize Strategy.* PhD thesis, Singapore-MIT Alliance, Nanyang Technological University, Singapore, 2003.

[2] B. O. Almroth, P. Stern, and F. A. Brogan. Automatic choice of global shape functions in structural analysis. *AIAA Journal*, 16:525–528, May 1978.

[3] E. Balmes. Parametric families of reduced finite element models: Theory and applications. *Mechanical Systems and Signal Processing*, 10(4):381–394, 1996.

[4] E. Barkanov. Transient response analysis of structures made from viscoelastic materials. *Int. J. Numer. Meth. Engng.*, 44:393–403, 1999.

[5] M. Barrault, N. C. Nguyen, Y. Maday, and A. T. Patera. An "empirical interpolation" method: Application to efficient reduced-basis discretization of partial differential equations. *C. R. Acad. Sci. Paris, Série I.*, 339:667–672, 2004.

[6] G. Caloz and J. Rappaz. Numerical analysis for nonlinear and bifurcation problems. In P.G. Ciarlet and J.L. Lions, editors, *Handbook of Numerical Analysis, Vol. V*, Techniques of Scientific Computing (Part 2), pages 487–637. Elsevier Science B.V., 1997.

[7] H. W. Engl, M. Hanke, and A. Neubauer. *Regularization of Inverse Problems.* Kluwer Academic, Dordrecht, 1996.

[8] J. P. Fink and W. C. Rheinboldt. On the error behavior of the reduced basis technique for nonlinear finite element approximations. *Z. Angew. Math. Mech.*, 63:21–28, 1983.

[9] M. D. Gunzburger. *Finite Element Methods for Viscous Incompressible Flows: A Guide to Theory, Practice, and Algorithms.* Academic Press, Boston, 1989.

[10] S. I. Ishak, G. R. Liu, S. P. Lim, and H. M. Shang. Locating and Sizing of Delamination in Composite Laminates Using Computational and Experimental Methods. *Composite Part B*, 32(4):287–298, 2001.

[11] K. Ito and S. S. Ravindran. A reduced basis method for control problems governed by PDEs. In W. Desch, F. Kappel, and K. Kunisch, editors, *Control and Estimation of Distributed Parameter Systems*, pages 153–168. Birkhäuser, 1998.

[12] K. Ito and S. S. Ravindran. A reduced-order method for simulation and control of fluid flows. *Journal of Computational Physics*, 143(2):403–425, July 1998.

[13] G. R. Liu and S. C. Chen. Flaw Detection in Sandwich Plates Based on Time-Harmonic Response Using Genetic Algorithm. *Comput. Methods Appl. Mech. Engrg.*, 190(42):5505–5514, August 2001.

[14] G. R. Liu, X. Han, and K. Y. Lam. A Combined Genetic Algorithm and Nonlinear Least Squares Method for Material Characterization Using Elastic Waves. *Comput. Methods Appl. Mech. Engrg.*, 191:1909–1921, 2002.

[15] G. R. Liu and K. Y. Lam. Characterization of a Horizontal Crack in Anisotropic Laminated Plates. *International Journal of Solids and Structures*, 31(21):2965–2977, 1994.

[16] G. R. Liu, K. Y. Lam, and J. Tani. Characterization of Flaws in Sandwich Plates: Numerical Experiment. *JSME International Journal (A), Japan*, 38(4):554–562, 1995.

[17] G. R. Liu, Z. C. Xi, K. Y. Lam, and H. M. Shang. A Strip Element Method for Analyzing Wave Scattering by a Crack in an Immersed Composite Laminate. *Journal of Applied Mechanics*, 66:898–903, 1999.

[18] L. Machiels, Y. Maday, I. B. Oliveira, A. T. Patera, and D. V. Rovas. Output bounds for reduced-basis approximations of symmetric positive definite eigenvalue problems. *C. R. Acad. Sci. Paris, Série I*, 331(2):153–158, July 2000.

[19] Y. Maday, A. T. Patera, and G. Turinici. Global *a priori* convergence theory for reduced-basis approximation of single-parameter symmetric coercive elliptic partial differential equations. *C. R. Acad. Sci. Paris, Série I*, 335(3):289–294, 2002.

[20] B.C. Moore. Principal component analysis in linear systems: controllability, observability, and model reduction. *IEEE Transactions on Automatic Control*, 26(1):17–32, 1981.

[21] N. C. Nguyen, K. Veroy, and A. T. Patera. Certified real-time solution of parametrized partial differential equations. In *Handbook of Materials Modeling*. Kluwer Academic Publishing, 2004. To appear.

[22] A. K. Noor and J. M. Peters. Reduced basis technique for nonlinear analysis of structures. *AIAA Journal*, 18(4):455–462, April 1980.

[23] I. B. Oliveira and A. T. Patera. Reduced-basis techniques for rapid reliable optimization of systems described by parametric partial differential equations. *Submitted, Optimization and Engineering.*

[24] J. S. Peterson. The reduced basis method for incompressible viscous flow calculations. *SIAM J. Sci. Stat. Comput.*, 10(4):777–786, July 1989.

[25] T. A. Porsching. Estimation of the error in the reduced basis method solution of nonlinear equations. *Mathematics of Computation*, 45(172):487–496, October 1985.

[26] T. A. Porsching and M. Lin Lee. The reduced basis method for initial value problems. *SIAM Journal on Numerical Analysis*, 24(6):1277–1287, 1987.

[27] C. Prud'homme, D. Rovas, K. Veroy, Y. Maday, A. T. Patera, and G. Turinici. Reliable real-time solution of parametrized partial differential equations: Reduced-basis output bound methods. *Journal of Fluids Engineering*, 124(1):70–80, March 2002.

[28] A. Quarteroni and A. Valli. *Numerical Approximation of Partial Differential Equations.* Springer, 2nd edition, 1997.

[29] B. Roux, editor. *Numerical Simulation of Oscillatory Convection in Low-Pr Fluids: A GAMM Workshop*, volume 27 of *Notes on Numerical Fluids Mechanics.* Vieweg, 1990.

[30] D.V. Rovas. *Reduced-Basis Output Bound Methods for Parametrized Partial Differential Equations.* PhD thesis, Massachusetts Institute of Technology, Cambridge, MA, October 2002.

[31] L. Sirovich. Turbulence and the dynamics of coherent structures, part 1: Coherent structures. *Quarterly of Applied Mathematics*, 45(3):561–571, October 1987.

[32] A. C. Skeldon, D. S. Riley, and K. A. Cliffe. Convection in a low Prandtl number fluid. *Journal of Crystal Growth*, 162:95–106, 1996.

[33] G. Talenti. Best constant in Sobolev inequality. *Ann. Mat. Pura Appl.*, 110(4):353–372, 1976.

[34] K. Veroy and A. T. Patera. Certified real-time solution of the parametrized steady incompressible Navier-Stokes equations; Rigorous reduced-basis *a posteriori* error bounds. *International Journal for Numerical Methods in Fluids*, 2004. To appear.

[35] K. Veroy, C. Prud'homme, and A. T. Patera. Reduced-basis approximation of the viscous Burgers equation: Rigorous *a posteriori* error bounds. *C. R. Acad. Sci. Paris, Serie I*, 337(9):619–624, November 2003.

[36] K. Veroy, C. Prud'homme, D. V. Rovas, and A. T. Patera. *A posteriori* error bounds for reduced-basis approximation of parametrized noncoercive and nonlinear elliptic partial differential equations (AIAA Paper 2003-3847). In *Proceedings of the 16th AIAA Computational Fluid Dynamics Conference*, June 2003.

8 Personnel Supported

Anthony T. Patera (principal investigator)
Martin A. Grepl (doctoral student)

9 Interactions

Meetings, conferences, and seminars.

- A.T. Patera. March 2004. Certified Real-Time Solution of the Parametrized Incompressible Navier-Stokes Equations. ICFD (Institute for Computational Fluid Dynamics) Conference on Numerical Methods for Fluid Dynamics, St. Catherine's College, Oxford, UK.
- A.T. Patera. May 2004. Certified Rapid Solution of Parametrized Partial Differential Equations for Real-Time Applications. 2nd Sandia Workshop of PDE-Constrained Optimization: Toward Real-Time and On-Line PDE-Constrained Optimization, Santa Fe, NM.
- M.A. Grepl and A.T. Patera. June 2004. Reduced-Basis Approximation of Parametrized Time-Dependent Partial Differential Equations: Application to Optimal Control. 6th INternational Conference on Spectral and High-Order Methods (ICOSAHOM '04), Brown University, RI.
- K. Veroy and A.T. Patera. February 2005. Reduced-Basis Approximation and Rigorous A Posteriori Error Estimators for compressible Navier-Stokes: Applicaiton to National Convection Problems. SIAM Conference on Computational Science and Engineering, Orlando, FL.

Other collaborators. Mathematical aspects of this work were performed in collaboration with Professor Y Maday (University of Paris VI); certain methodologies for certified real-time parameter estimation were developed in collaboration with NC Nguyen and Professor GR Liu (both of National University of Singapore), Dr C Prud'homme (EPFL), and Dr K Veroy (MIT); and optimization formulations benefited from the participation of Professor D Bertsimas and Mr K-M Teo (both of MIT). Dr D Backman and Dr D Wei (both of GE) were also crucial in helping us understand certain important application contexts.

10 Publications Resulting from this Research

The following papers have resulted directly from this research:

- N.C. Nguyen, K. Veroy, and A.T. Patera. Certified real-time solution of parametrized partial differential equations, in Handbook of Materials Modeling, Kluwer Academic Publishing, 2004. To appear.
- K. Veroy and A.T. Patera. Certified real-time solution of the parametrized steady incompressible Navier-Stokes equation; Rigerous reduced-basis a posteriori error bounds, International Journal for Numerical Methods in Fluids, 2004. To appear.
- M.A. Grepl and A.T. Patera, A posteriori error bounds for reduced-basis approximaiton of parameterized parabolic partial differential equations, M2AN (Math. Mod. Numer. Anal.), 2004. To appear.
- M.A. Grepl, N.C. Nguyen, K. Veroy, A.T. Patera, and G.R. Liu, Certified Rapid Solution of Parametrized Partial Differential Equations for Real-Time applications. Proceedings of the 2nd Sandia Workshop of PDE-Constrained Optimization: Towards Real-Time and On-Line PDE-Constrained Optimization, SIAM Computational Science and Engineering Book Series. Submitted 2004.

Project 3 — Computing Bounds for Functional Output of Solutions of PDE's

Project 3(a):

Computing Bounds for Functional Output of Solutions of PDE's

Investigator: Jaime Peraire
Department of Aeronautics and Astronautics
Room 37-451
Massachusetts Institute of Technology
Cambridge, MA 02139

Background: Exact Bounds and Certificates

Existing techniques for approximating the solutions of PDE's rely on the experience of the user to estimate a-priori the size of the discretization required to resolve the various problem features. Failure to appropriately do so, may result in results which are either too expensive to obtain or, worse yet, uncertain. Modern a-posteriori and mesh adaptivity methods have the potential to alleviate this problem, but not to eliminate it completely, i.e. a saturation hypothesis needs to be made that can not be verified a-priori.

For a number of years we have been engaged in the development of techniques for computing strict bounds for functional outputs of the exact solution of partial differential equations. Our approach draws on previous work on a-posterior error estimation and complementary energy ideas well known in the mechanics community. We have generalized the previous work in a number of ways. Relative to existing a-posteriori error estimation techniques, our approach delivers bounds with respect to the exact solution of the PDE as opposed to just an estimate of the computed error. Relative to the complementary energy methods, which are only capable of delivering bounds for the energy in problems for which a variational principle exists, we are able to handle general linear outputs, some non-linear outputs, and some non-symmetric problems both linear and non-linear for which variational principles may not exist.

The starting point for our bounds procedure is a finite element approximation to the solution and to the output dependent adjoint solution. These approximations are then post-processed to yield the so called inter-element hybrid fluxes. The hybrid fluxes are then used as data for the computation of locally equilibrated stress fields. The final expression for the bounds is obtained by calculating appropriate norms of the stress fields. It is shown that the computed bounds are uniformly valid regardless of the size of the underlying coarse discretization, but as expected, their sharpness depends on the accuracy of the approximated solutions. A mesh adaptive procedure has also been developed which can be used to determine the bounds to a preset level of accuracy.

An attractive feature of our approach is that the piecewise polynomial equilibrated stress-like fields, which are computed as part of the bound process, can be used as certificates to guarantee the correctness of the computed bounds. It turns out that given a stress field, it is easy to check whether this field corresponds to a valid certificate, and in the affirmative case, it is straightforward to determine the value of the output that it can certify. In particular, the stress fields need to satisfy continuity of normal tractions across elements, and membership of an appropriate space.

The idea of a certificate that is computed simultaneously with the solution has many attractive features. In particular, a certificate consisting of the data set necessary to describe the piecewise

polynomial stress-like fields could be used to document the computed results. We note that exercising the certificate does not require access to the code used to compute it, and can be done with a simple algorithm which does not require solving a system of equations. A very important point is that, if a certificate meets all the necessary conditions, which in turn are easy to verify, then, there is no need to certify the code used to compute it. In practice, the size of these certificates depends on the required level of certainty. As expected, we shall find that high levels of certainty, i.e. small bound gaps, will often require longer certificates (larger data sets) than those required to certify less sharp claims.

To date, we have been successful at developing algorithms for computing bounds for:

- Linear Functional Outputs of the Convection-Diffusion-Reaction Equation
- Linear Functional Outputs of the Linear Elasticity Equations
- Energy Release Rates (J-Integral) in Linear Elasticity
- Linear Functional Outputs for the Stokes Equation

1 Particular Achievements

The focus of this project has been the extension of our methodology to the computation of strict upper and lower bounds for for the collapse load in limit analysis.

Limit analysis is relevant in many practical engineering areas such as the design of mechanical structures or the analysis of pressurized vessels. Whereas linear elastic analyses are typically used to determine the performance of the structure (usually characterized by deflections) under the so called service loads, limit analysis is used to determine the collapse load. Assuming a rigid, perfectly-plastic solid subject to a static load distribution, the problem of limit analysis consists of finding the minimum multiple of this load distribution that will cause the body to collapse. This collapse multiplier results from solving an infinite dimensional saddle point problem, where the internal work rate is maximized over an admissible set of stresses -defined by a yield condition- and minimized over the linear space of kinematically admissible velocities for which the external work rate equals the unity. When strong duality is applied to this saddle point problem, the well-known convex (and equivalent) static and kinematic principles of limit analysis arise. In this project, an efficient procedure to compute strict upper and lower bounds for the exact collapse multiplier has been developed, with a formulation that explicitly considers the exact convex yield condition. The approach consists of two main steps. First, the continuous problem, under the form of the static principle, is discretized twice (one per bound) by means of different combinations of finite element spaces for the stresses and velocities. For each discretization, the interpolation spaces are chosen so that the attainment of an upper or a lower bound is guaranteed. The second step consists of solving the resulting discrete nonlinear optimization problems. Towards this end, they are reformulated into the canonical form of Second-order Cone Programs, which allows for the use of primal-dual interior point methods that optimally exploit the convexity and duality properties of the limit analysis model and guarantee global convergence to the optimal solutions. To exploit the fact that collapse mechanisms are typically highly localized, a novel method for adaptive meshing is introduced based on local bound gap measures and not on heuristic estimates. The method decomposes the total bound gap as the sum of positive elemental contributions from each element in the mesh, and refines only those elements which are responsible for the majority of the numerical error. Finally, stand-alone computational certificates that allow the bounds to be verified independently, without

recourse to the original computer program, are also provided. This removes the uncertainty about the reliability of the results, which frequently undermines the utility of computational simulations.

1.1 Application Example

For illustration purposes, we show two computations on the same geometry. One is carried out using a linear elastic model and the other one carried out using limit state analysis. The figure below shows a square thin plate with two rectangular cut-outs. The plate is loaded with a uniform traction on its boundary, and as a consequence, the material develops a strain induced stresses. Due to symmetry only one quarter of the plate is analyzed.

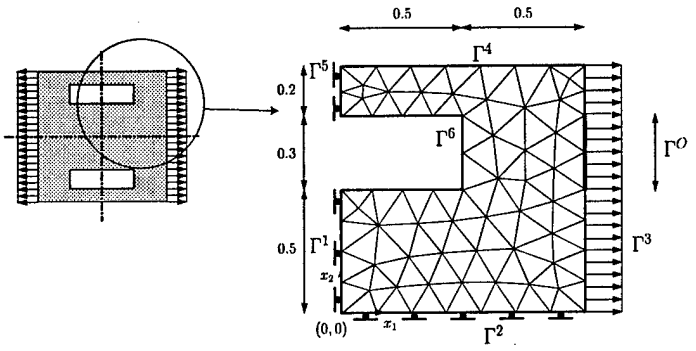

Figure 1: Thin square plate with rectangular holes under a plane stress loading.

1.1.1 Linear Elastic Analysis

In this case, we are interested in the maximum displacement that the portion of the boundary Γ^O would experience as a result of the loading. Therefore, our output of interest becomes the average horizontal displacement over Γ^O. The figure below shows the sequence of adapted meshes automatically generated during this computation. The table shows the lower and upper bounds computed, $s_{\pm}$, as well as the bound gap, Δ, as a function of the number of elements in the mesh. We point out that this bounds are strict with respect to the analytical solution of the problem and that a certificate for these computations could be easily generated.

n_{el}	108	222	433	811	1387	1966	2532	3069	3564
Δ	.1074	.1821	.1217	.0719	.0375	.0242	.0157	.0117	.0083
s_+	.3695	.3894	.3688	.3508	.3375	.3339	.3292	.3282	.3262
s_-	.2620	.2072	.2470	.2789	.2999	.3096	.3134	.3165	.3179

Table 1: Computed bounds in a series of adaptively h-refined meshes.

1.1.2 Limit Analysis

Here, the problem is studied using the limit analysis theory. Given a yield criterion for the material (here the von Mises yield criterion has been used), we want to calculate the maximum load multiplier that can be applied to the plate before the plate collapses. The problem has been solved using the developed formulation and the SDP3T second order cone solver. It is worth noting that in this case the collapse mechanism consists of two localized shear bands which concentrate most of the deformation whereas the rest of the plate behaves very much like a rigid body. Below we

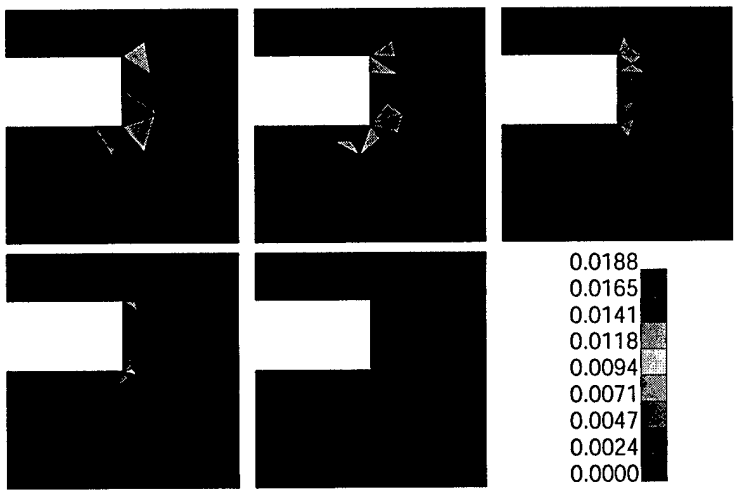

Figure 2: Sequence of adapted meshes for the average displacement output over Γ^O. Number of elements: 108, 165, 280, 405 and 538

illustrate the computed results. The left figure shows the contours of equal horizontal displacement, the middle figure shows the contours of equal effective deformation, and the right figure shows the convergence of the upper and lower bounds for the load multiplier, as the grid is refined.

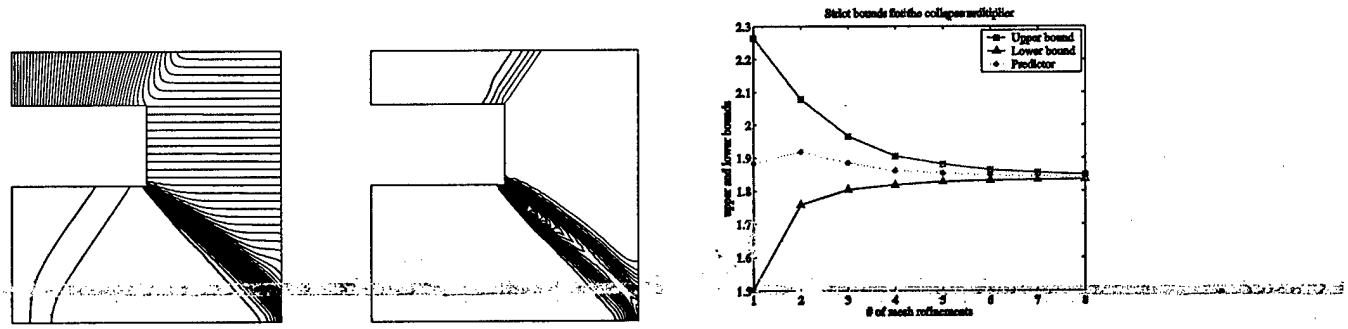

Figure 3: Contours of equal horizontal displacement, contours of equal effective deformation, and convergence of the upper and lower bounds for the load multiplier as the grid is refined.

2 Personnel Supported

The funds provided for this project were used to partially support H. Ciria during his S.M. degree. The title of his thesis is "Computation of Upper and Lower Bounds in Limit Analysis Using Second Order Cone Programming and Mesh Adaptivity"

3 Interactions

The work reported here involves numerous collaborations with other research groups as well as institutions. The idea of certification of computational results is of direct interest to the research group at Sandia National Laboratories with which we have a longstanding collaboration. The work developed under this project has been presented at conferences and meetings over the last year

and the initial feedback has been positive. At the personal level, we have interacted closely with Professors A.T. Patera and P. Parrilo from MIT, A. Huerta and N. Pares from UPC, Barcelona, J. Bonet from UC Swansea, and K.C. Toh from NUS.

4 Publications Resulting from this Research

The following papers have resulted directly from this research:

- H. Ciria and J. Peraire, Computation of Upper and Lower Bounds in Limit State Analysis using Second-Order Cone Programming and Mesh Adpativity, presented at the 9th ASCE Speciality Conference on Probabilistic Mechanics and Structural Reliability, June 2004, Albuquerque.
- H. Ciria and J. Peraire, Upper and Lower Bounds in Limit State Analysis using a Second-Order Cone Programming Formulation, in preparation.
- H. Ciria, J. Bonet and J. Peraire, Mesh Adaptive Algorithm for Limit State Analysis, in preparation

The following papers are related to this research. They present rigorous upper and lower bound algorithms for different classes of equations:

- Sauer-Budge A.M., Bonet J., Huerta A., Peraire J., Computing bounds for linear functionals of exact weak solutions to Poisson's equation, *SIAM Journal on Numerical Analysis*, Vol 42, 4, 1610-1630, 2004.
- Sauer-Budge A.M., Peraire J., Computing bounds for linear functionals of exact weak solutions to the advection-diffusion-reaction equation, *SIAM Journal on Scientific Computing*, Vol 26, 2, 636-652, 2004.
- Pares N., Bonet J., Huerta A., Peraire J. The computation of bounds for linear-functional outputs of weak solutions to the two-dimensional elasticity equations, submitted to Comp. Meths. Appl. Mech. Engr. 2004.
- Xuan Z.C., Lee K.H., Patera A.T., Peraire J., Computing upper and lower bounds for the J-integral in two-dimensional linear elasticity, SMA Symposium, January 2004.
- Xuan Z.C., Pares N., Peraire J., Computing upper and lower bounds for energy release rates in linear elasticity, submitted to Comp. Meths. Appl. Mech. Engr., 2004.

5 Future Work

We feel that this research can be extended in a number of meaningful ways. In particular, we are looking into deformation-plasticity constitutive models which can be interpreted as a generalization of the linear elastic and limit analysis theories. To our knowledge, no methods have been proposed which are able to deliver bounds for these types of theories.

Project 3(b):

Bounds on Functional Outputs and Semidefinite Programming[2]

Investigator: John C. Doyle
Control and Dynamical System 107-81
1200 E. California Blvd.
California Institute of Technology
Pasadena, CA 91125

Our work in this area has concentrated on the algorithmic construction of Lyapunov-like functions that certify upper and lower bounds on functional outputs of PDEs. These functions are a generalization of barrier functions for ODEs [5], a framework that can be used to answer many analysis-type questions in systems theory, such as model invalidation based on data and hybrid system verification [6]. Apart from the problem of estimating functional outputs, we have also tackled the problem of assessing stability of steady-states of parabolic PDEs through the construction of Lyapunov functions. Both results have shown that semidefinite programming in general and sum of squares in particular open new, unexplored possibilities and provide a unique perspective for future research in systems described by Partial Differential Equations. A technical paper is currently under preparation.

1 Estimating bounds for functional outputs

We have developed techniques for computing upper and lower bounds on functional outputs for all three types of PDEs — elliptic, parabolic and hyperbolic — in their standard form with forcing terms and the necessary boundary and initial conditions. The functional outputs may be spatial and/or temporal averages of the state or functions of state of the system.

In particular we developed two methodologies that are complementing each other in many respects. First, for elliptic and parabolic type PDEs we use the maximum principle to estimate functional outputs. For PDEs where the maximum principle does not hold, barrier certificates can be used instead. Here we outline these two techniques through illustrative examples. In a later section, we concentrate on the issue of assessing stability of steady-states for PDEs, through the construction of Lyapunov-type certificates.

1.1 PDEs with a 'maximum' principle

This method resembles the method of subharmonics in Perron's process [3], and is valid for elliptic and parabolic PDEs. It is based on the construction of approximations to the true solution. To illustrate the technique, consider a 1-D Poisson equation defined in a region $\Omega = [0, 1]$:

$$\frac{d^2u}{dt^2} = f, \quad u(0) = A_0, \quad u(1) = A_1.$$

Suppose the output functional $y = \int_0^1 u dt$ needs to be estimated. To do this, we search for a polynomial function $B(t)$ so that

$$\frac{d^2B}{dt^2} - f \leq 0, \quad \int_0^1 B(t)dt - \gamma \leq 0, \quad B(0) = A_0, \quad B(1) = A_1$$

[2]Written by Antonis Papachristodoulou. Email: antonis@cds.caltech.edu

The first condition guarantees that $B(t) \geq u(t)$; the second condition imposes $\int_0^1 u(t)dt \leq \int_0^1 B(t)dt \leq \gamma$ and therefore a good upper bound can be obtained as the order of B is increased and γ is optimized. Lower bounds can also be obtained by changing the direction of the inequalities in the above conditions.

The non-negativity conditions that the function B has to satisfy can be relaxed to the existence of a sum of squares decomposition; using SOSTOOLS [7], such functions can be constructed and upper and lower bounds on y can be estimated. The same technique can be used for parabolic equations which satisfy the maximum principle.

The disadvantage of this technique is that the output functional has to be *linear* in the unknown coefficients of u, for otherwise the problem is not convex anymore and semidefinite programming cannot be used directly to construct the functions B. Moreover for hyperbolic equations, this technique cannot be used. To tackle these two cases, we introduced the method of barrier certificates.

1.2 Using barriers to the solution

This methodology centers on disproving that certain bounds can be obtained, by constructing appropriate state-barrier functions. More theory can be found in [5], where the problem of model invalidation based on data is tackled. In particular, consider a system of the form:

$$\frac{dx}{dt} = f(x,t), \quad x(t_0) = x_0 \tag{1}$$

where $x \in \mathcal{X} \subset \mathbb{R}^n$ and f is such that solutions exist and are unique in $\mathcal{X}$. Suppose we wanted to disprove that at time t_f, the solution $x_f \in \mathcal{X}_f$ can never be achieved. This can be done by exhibiting a function $B(x,t)$ with the following properties:

$$\begin{aligned} B(x_f,t_f) - B(x_0,t_0) &> \epsilon, \qquad \text{for } x_f \in \mathcal{X}_f, \quad \epsilon > 0 \\ \frac{dB}{dt} = \frac{\partial B(x,t)}{\partial t} + \frac{\partial B(x,t)}{\partial x} f(x,t) &\leq 0, \qquad \text{for } t \in [t_0,t_1], \quad x \in \mathcal{X}. \end{aligned}$$

The first condition ensures that B at the final time has a value that is strictly greater than at the initial time, whereas the second condition ensures the opposite: that B decreases as the system evolves. Therefore the set $\mathcal{X}_f$ can never be reached. To use the above result algorithmically, we first capture the sets $\mathcal{X}$ and $\mathcal{X}_f$ by a set of inequalities. To verify the above conditions, we use two tools: the S-procedure (a generalization of the Lagrange multiplier method in optimization) to adjoin these inequalities to the corresponding conditions; and the sum of squares decomposition and SOSTOOLS to construct B algorithmically.

The above methodology has been fully developed for systems described by Ordinary Differential Equations. In this section we will use this technique to estimate functional outputs with more general kernels, and treat the wave equation. Consider first the one-dimensional Poisson's equation

$$\frac{d^2u}{dt^2} = f \text{ for } t \in [t_0,t_1], \quad u(t_0) = A_0, \quad u(t_1) = A_1.$$

Let the functional output to be estimated be

$$y(t_1) = \int_{t_0}^{t_1} \left(\left| \frac{du}{dt} \right|^2 - 2fu \right) dt$$

It is easy to verify that the above setup is equivalent to

$$\frac{d}{dt} \begin{bmatrix} u_1 \\ u_2 \\ u_3 \end{bmatrix} = \begin{bmatrix} u_2 \\ f \\ u_2^2 - 2fu_1 \end{bmatrix}, \quad y = u_3(t_1), \quad u_1(t_0) = A_0, \quad u_3(t_0) = 0, \quad u_1(t_1) = A_1.$$

We have thus turned our problem into the aforementioned standard form. Now, we can postulate appropriate regions $\mathcal{X}_f$ to be disproved, yielding upper and lower bounds on $u_3(t_1)$.

The case of the 1-D wave equation can be treated in the same way. Let

$$\frac{d^2u}{dt^2} + k^2u = f, \quad t \in [t_0, t_1], \quad \dot{u}(t_0) = A_0, \quad u(t_1) = A_1$$

Let the output condition be

$$y(t_1) = \int_{t_0}^{t_1} u dt$$

The above is equivalent to

$$\frac{d}{dt}\begin{bmatrix} u_1 \\ u_2 \\ u_3 \end{bmatrix} = \begin{bmatrix} u_2 \\ -k^2u_1 + f \\ u_1 \end{bmatrix}, \quad y = u_3(t_1), \quad u_1(t_0) = a_0, \quad u_3(t_0) = 0, \quad u_1(t_1) = a_1.$$

Again the system is in the standard form and upper and lower bounds can be estimated directly.

The question that emerges is whether PDEs in more variables can be treated. To do this, we need to generalize the notion of barrier functions to the notion of barrier functionals. The complication is superficial; for example, consider the one-way wave equation

$$u_t = u_x + tx(\pi - x), \quad u(0,t) = 0, \quad u(\pi,t) = 0, \quad u(x,0) = 0.$$

Suppose we wanted to estimate:

$$v(0.5) = \int_0^\pi u(x, 0.5)dx$$

Here, we can construct a functional of the form:

$$B(v,t) = a_0(t) + a_1(t)\int_0^\pi u dx + a_2(t)\left(\int_0^\pi u dx\right)^2 + \dots \tag{2}$$

Now we have:

$$\frac{dB}{dt} = \frac{\partial B}{\partial t} + a_1(t)\int_0^\pi u_t dx + 2a_2(t)\int_0^\pi u dx \int_0^\pi u_t dx + \dots$$

From the describing equation, through integration by parts we get $\int_0^\pi u_t dx = \frac{\pi^3}{6}t$. The barrier methodology can be applied to this case directly, through which we can get upper and lower bounds on $\int_0^\pi u(x, 0.5)dx$ that converge to the true value of 0.6296.

The same technique can be used to analyze other types of PDEs, even nonlinear. Consider for example Burger's equation:

$$u_t + uu_x = \nu u_{xx}, \quad u(0,t) = 1, \quad u(1,t) = 0, \quad u(x,0) = 1 - x.$$

Suppose we were interested in a bound on the value of $\frac{\partial u}{\partial x}$ at $x = 1$ at a specified or at an infinite time horizon. Consider a function of the form (2). Then it is easy to see that now

$$\int_0^1 u_t dx = \nu u_x|_0^1 - \frac{1}{2}.$$

Using B as a barrier function, we can estimate the value of $\nu u_x|_0^1$. With our data this value is 0.5, which is what the upper and lower values obtained using the barrier method give.

2 Stability analysis of systems described by PDEs

Our work on the algorithmic construction of barrier functionals to estimate functional outputs for PDEs was motivated by the related issue of stability analysis of infinite dimensional systems [4, 2, 1]. For this, we used a methodology based on the construction of *functional certificates* of integral type whose kernels are polynomials. The construction is done using semidefinite programming and SOSTOOLS.

Stability notions for systems described by PDEs can be found in [2]. Through a careful definition of a *nonlinear system* (semigroup) $S(t)$ on a complete metric space C with metric ρ and the orbit through a point x in this space, one defines what is an *equilibrium point.* Stability is then defined through an ϵ-δ argument, under the above metric, and to ensure it, one can construct a Lyapunov function, i.e. continuous real-valued function V on C such that

$$\dot{V}(x) \triangleq \overline{\lim}_{t\to 0+} \frac{1}{t}\{V(S(t)x) - V(x)\} \leq 0$$

for all $x \in C$, not excluding the possibility $\dot{V}(x) = -\infty$. The Lyapunov stability theorem is similar to the one in finite dimensions, and reads

Theorem 1 *(Lyapunov theorem) [2] Let $\{S(t), t \geq 0\}$ be a dynamical system on C, and let 0 be an equilibrium point in C. Suppose V is a Lyapunov function which satisfies $V(0) = 0$, $V(x) \geq c(\|x\|)$ for $x \in C$, $\|x\| = \rho\{x, 0\}$, where $c(\cdot)$ is a continuous strictly increasing function, $c(0) = 0$ and $c(r) > 0$ for $r > 0$. Then 0 is stable. If in addition $\dot{V}(x) \leq -c_1(\|x\|)$ where $c_1(\cdot)$ is also continuous, increasing and positive with $c_1(0) = 0$, then 0 is asymptotically stable.*

Although there is a converse theorem, finding a Lyapunov function in any particular case is usually difficult, especially finding one that satisfies all the above requirements. Instead, the sum of squares decomposition can be used to construct them algorithmically.

Consider for example the system

$$\begin{aligned} u_t &= u_{xx} + \rho u^3 + \alpha u \\ u(\pm 1, t) &= 0 \end{aligned} \tag{3}$$

with $\rho \leq 0$. From the linearization of this system about the zero steady state, stability is guaranteed for $\alpha < \pi^2/4$. Here we are interested in constructing the Lyapunov function

$$V(u) = \int_{-1}^{1} a(u(\eta, t), \eta) d\eta \tag{4}$$

where a is a polynomial in its arguments, of order at least 2 in u. When $\dot{V}$ is considered, the system dynamics come into play and through integration by parts of the resulting expression, the boundary conditions appear. In particular, the following 'by-product' conditions can be obtained

$$\int_{-1}^{1} \left\{ \frac{\partial a}{\partial u} u_{\eta\eta} + u_\eta^2 \frac{\partial^2 a}{\partial u^2} - u \left[\frac{\partial^3 a}{\partial u^2 \partial \eta} u_\eta + \frac{\partial^3 a}{\partial u_\eta \partial \eta^2} \right] \right\} d\eta = 0$$

as a result of integration by parts of the term $\int_{-1}^{1} \frac{\partial a}{\partial u} u_{\eta\eta} d\eta$. Also, we have used the fact that $u \frac{\partial^2 a}{\partial u \partial \eta}\Big|_{-1}^{1} = 0$ and the fact that $u_\eta \frac{\partial a}{\partial u}\Big|_{-1}^{1} = 0$ since a is a polynomial of degree at least 2 in u. Notice that the following is also true:

$$\int_{-1}^{1} \eta^n u^2 d\eta = -\int_{-1}^{1} n\eta^n u^2 d\eta - 2\int_{-1}^{1} \eta^{n+1} u u_\eta d\eta$$

i.e.

$$\int_{-1}^{1} \left[(1+n)\eta^n u^2 + 2\eta^{n+1} u u_\eta\right] d\eta = 0$$

Stability in L_2 can then be guaranteed by constructing a polynomial $a(u,\eta)$ and a positive definite function φ such that the following hold:

1. $a(u,\eta) - \varphi(u) \geq 0$ when $\eta \in [-1,1]$,
2. $-\alpha\frac{\partial a}{\partial u}u - u_\eta^2\frac{\partial^2 a}{\partial u^2} + u\left[\frac{\partial^3 a}{\partial u^2 \partial \eta}u_\eta + \frac{\partial^3 a}{\partial u_\eta \partial \eta^2}\right] - \epsilon u^2 \geq 0$ when $\eta \in [-1,1]$ and $(1+n)\eta^n u^2 + 2\eta^{n+1} u u_\eta = 0$ is satisfied.

This is because the two conditions guarantee the existence of a Lyapunov functional, given by (4), that is positive definite and whose derivative is negative definite. Numerical tests show that as the order of a with respect to η is increased, the conservativeness in the bounds obtained is reduced.

References

[1] S. P. Banks. *State-space and frequency-domain methods in the control of distributed parameter systems.* Peter Peregrinus Ltd., London, UK, 1983.

[2] D. Henry. *Geometric Theory of semilinear parabolic equations.* Springer-Verlag, Berlin, 1981.

[3] Fritz John. *Partial Differential Equations.* Springer-Verlag, New York, 1982.

[4] A. Pazy. *Semigroups of Linear Operators and Applications to Partial Differential Equations.* Springer-Verlag, Berlin, 1983.

[5] S. Prajna. Barrier certificates for nonlinear model validation. In *Proceedings IEEE Conference on Decision and Control*, 2003.

[6] S. Prajna and A. Jadbabaie. Safety verification of hybrid systems using barrier certificates. In *Hybrid Systems: Computation and Control.* Springer-Verlag, 2004.

[7] S. Prajna, A. Papachristodoulou, and P. A. Parrilo. SOSTOOLS – Sum of Squares Optimization Toolbox, User's Guide. Available at `http://www.cds.caltech.edu/sostools` and `http://www.aut.ee.ethz.ch/~parrilo/sostools`, 2002.